STATIC AEROELASTIC ANALYSIS OF A GENERIC SLENDER MISSILE USING A LOOSELY COUPLED FLUID STRUCTURE INTERACTION METHOD

A THESIS SUBMITTED TO
THE GRADUATE SCHOOL OF NATURAL AND APPLIED SCIENCES
OF
MIDDLE EAST TECHNICAL UNIVERSITY

BY

MEHMET AKGÜL

IN PARTIAL FULFILLMENT OF THE REQUIREMENTS
FOR
THE DEGREE OF MASTER OF SCIENCE
IN
MECHANICAL ENGINEERING

FEBRUARY 2012

Approval of the thesis

STATIC AEROELASTIC ANALYSIS OF A GENERIC SLENDER MISSILE USING A LOOSELY COUPLED FLUID STRUCTURE INTERACTION METHOD

Submitted by **MEHMET AKGÜL** in partial fulfillment of the requirements for the degree of **Master of Science in Mechanical Engineering Department, Middle East Technical University** by**,**

Prof. Dr. Canan ÖZGEN _____
Dean, Graduate School of **Natural and Applied Sciences**

Prof. Dr. Suha ORAL _____
Head of Department, **Mechanical Engineering**

Assist. Prof. Dr. Cüneyt SERT _____
Supervisor, **Mechanical Engineering Dept., METU**

Examining Committee Members:

Prof. Dr. Kahraman ALBAYRAK _____
Mechanical Engineering Dept., METU

Assist. Prof. Dr. Cüneyt SERT _____
Mechanical Engineering Dept., METU

Assist. Prof. Dr. Yiğit YAZICIOĞLU _____
Mechanical Engineering Dept., METU

Assist. Prof. Dr. M. Metin YAVUZ _____
Mechanical Engineering Dept., METU

Ali AKGÜL, M.Sc. _____
Chief Engineer, ROKETSAN

Date: 09/02/2012

I hereby declare that all the information in this document has been obtained and presented in accordance with academic rules and ethical conduct. I also declare that, as required by these rules and conduct, I have fully cited and referenced all material and results that are not original to this work.

Name, Last name : Mehmet AKGÜL

Signature :

ABSTRACT

STATIC AEROELASTIC ANALYSIS OF A GENERIC SLENDER MISSILE USING A LOOSELY COUPLED FLUID STRUCTURE INTERACTION METHOD

Akgül, Mehmet
M.Sc., Department of Mechanical Engineering
Supervisor: Assist. Prof. Dr. Cüneyt Sert

February 2012, 58 Pages

In this thesis, a loosely coupled Fluid-Structure Interaction (FSI) analysis method is developed for the solution of steady state missile/rocket aeroelastic problems. FLUENT is used as the Computational Fluid Dynamics (CFD) tool to solve Euler equations whereas ANSYS is used as the Computational Structural Dynamics (CSD) tool to solve linear structural problem. The use of two different solvers requires exchanging data between fluid and structure domains at each iteration step. Kriging interpolation method is employed for the data transfer between non-coincident fluid and structure grids. For mesh deformation FLUENT's built-in spring based smoothing approach is utilized. The study is mainly divided into two parts. In the first part static aeroelastic analysis for AGARD 445.6 wing is conducted and the results are compared with the reference studies. Deformation and pressure coefficient results are compared with reference both of which are in good agreement. In the second part, to investigate possible effects of aeroelasticity on rocket and missile configurations, static aeroelastic analysis for a canard controlled generic slender missile which is similar to a conventional 2.75" rocket geometry is conducted and results of the analysis for elastic missile are compared with the rigid case. It is seen that the lift force produced by canards and tails lessen due to deformations, stability characteristics of the missile decreases significantly and center of pressure location changes due to the deformations in the control surfaces.

Keywords: Fluid-Structure Interaction, FSI, Loosely Coupled Approach, Kriging Interpolation, AGARD 445.6 Wing, Slender Generic Missile, FLUENT, ANSYS

ÖZ

GEVŞEK BAĞLI BİR AKIŞKAN KATI ETKİLEŞİM YÖNTEMİ KULLANILARAK NARİN BİR FÜZENİN STATİK AEROELASTİK ANALİZLERİNİN YAPILMASI

Akgül, Mehmet
Yüksek Lisans, Makina Mühendisliği Bölümü
Tez Yöneticisi: Yrd. Doç. Dr. Cüneyt Sert

Şubat 2012, 58 Sayfa

Bu tezde, füze ve roket geometrileri için zamandan bağımsız akışkan katı etkileşimli analizler yapabilmek için gevşek bağlı akışkan katı etkileşimi analiz yöntemi geliştirilmiştir. Bu yöntemde Euler denklemlerinin çözümü için hesaplamalı akışkanlar dinamiği analiz aracı FLUENT, doğrusal yapısal katı probleminin çözümü için ise ANSYS yazılımı kullanılmıştır. Akışkan ve katı problemleri için iki farklı yazılımın kullanılması her çözüm adımında yazılımlar arası veri transferini zorunlu kılmaktadır. Birbiri ile örtüşmeyen akışkan ve katı çözüm ağları arasında veri alış-verişi için Kriging yöntemi, çözüm ağı hareketlerinin modellenmesinde ise FLUENT içerisinde yer alan yay bazlı düzgünleştirici aracı kullanılmaktadır. Çalışma temel olarak iki bölümden oluşmaktadır. İlk bölümde AGARD 445.6 kanadı için zamandan bağımsız akışkan katı etkileşimli analizleri gerçekleştirilmiş ve elde edilen sonuçlar referans sonuçlarla karşılaştırılmıştır. Bükülme ve basınç katsayısı değerleri karşılaştırıldığında sonuçların referans değerlerle örtüştüğü gözlemlenmektedir. İkinci kısımda ise füze ve roket konfigürasyonlarında akışkan katı etkileşimi etkilerini incelemek amacıyla kanard kontrollü, narinlik oranı yüksek füze geometrisi için zamandan bağımsız analizler yapılmış ve sonuçlar esnemez füze konfigürasyonu ile karşılaştırılmıştır. Bu analiz sonucunda kanatlardaki bükülmenin kaldırma

kuvvetini azalttığı, füze stabilitesinin düştüğü ve kontrol yüzeyleri üzerindeki basınç merkezi konumunun değiştiği görülmektedir.

Anahtar Kelimeler: Akışkan-Katı Etkileşimi, Gevşek Bağlı Yaklaşım, Kriging Enterpolasyonu, AGARD 445.6 Kanadı, Narinlik Oranı Yüksek Füze, FLUENT, ANSYS

To My Family

ACKNOWLEDGEMENTS

I wish my deepest gratitude to my supervisor Dr. Cüneyt Sert for his guidance, advice, criticism and encouragements throughout the thesis.

I also wish to thank my chief engineer Mr. Ali Akgül for his guidance and support during this study. I also would like to thank my colleagues in Aerodynamics Division of ROKETSAN for all their help and support during the thesis.

I am very thankful to my parents Mrs. Mahiye Akgül, Mr. Mahmut Akgül and my sisters Ms. Buket Akgül and Ms. Meltem Akgül for their help and motivation. Without them this work would not be completed.

I want to express my best wishes to Ms. Sezgi Bellek, Mr. Ekin Ağsarlıoğlu and Mr. Hayri Yiğit Akargün for their friendship and support during this study.

TABLE OF CONTENTS

LIST OF FIGURES

FIGURES

LIST OF TABLES

TABLES

CHAPTER 1

INTRODUCTION

Advances in computer technology and developments in numerical solutions to engineering problems lead engineers to work more frequently with computational fluid dynamics (CFD) and computational structural dynamics (CSD) analysis. Generally a CFD analysis is a sequential process of modeling the geometry, defining the flow region and flow conditions, solving the fluid flow in the described flow region and postprocessing the results. In such analyses the geometry is usually assumed as rigid which is not necessarily the case. In real world, fluid motion generates forces on structures, structures deform due to these forces and fluid motion is affected by structural deformations which results in new forces and this interaction loop goes on.

The rigid geometry assumption holds for many engineering problems. But in some cases, where the structure is flexible, fluid-structure interaction becomes important. Aircraft wing flutter, simulation of aortic valve and wind effects on suspension bridges, in which flexible structures are present, are some of the engineering problems that the rigid body assumptions may not work. Especially in aerospace applications fluid-structure interaction becomes very critical since flexible and light structures are present in all aerial vehicles which are the main concern of this thesis.

Usually in aerodynamic design processes, rigid fins and bodies are tested or analyzed and desired aerodynamic loads are obtained for stationary flow conditions. However in real life rigidity conditions cannot go beyond approximations due to the weight and aerodynamic design criteria. All the nonlinearities that decrease the rigidity of

the structure are difficult to determine and predict. In a multidisciplinary design process that includes aerodynamic and structural design all of these difficulties should be considered [1]. In such a multidisciplinary design wind tunnel and flight tests can be used as design tools. But the use of these facilities is expensive and time consuming. A cheaper and faster solution is needed for a multidisciplinary design phase in which solution of fluid-structure interaction problems is required. Developments in computer technology made it possible to bring numerical solutions to fluid-structure interaction problems. But solving fluid-structure interaction problems brought its own difficulties with it.

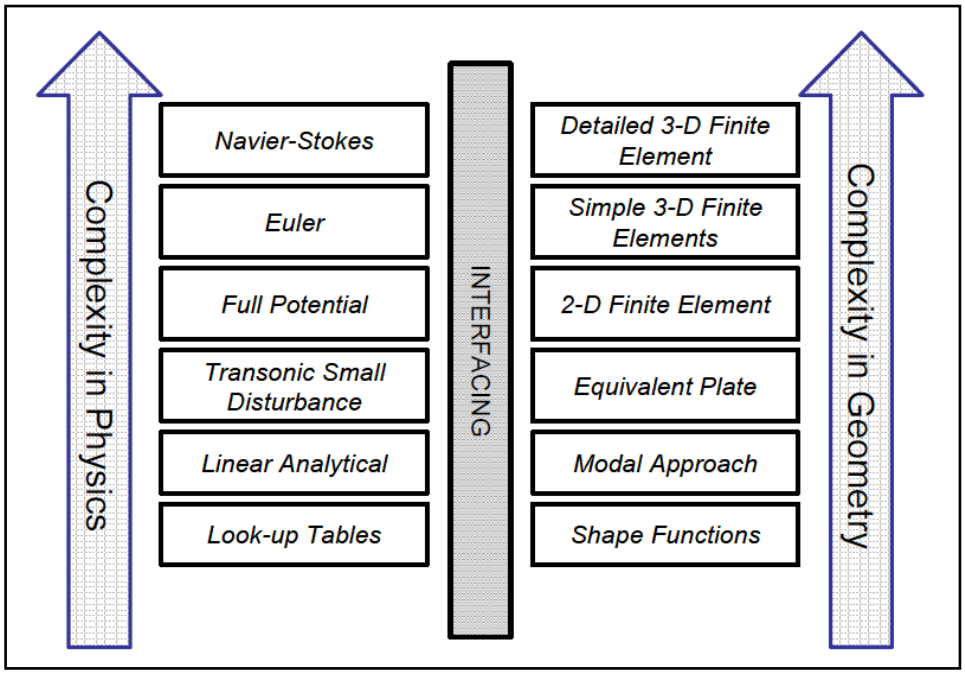

Figure 1-1 Solution domain complexity [2]

Also solution of the fluid or structural domain can be modeled according to the complexity of the problem. Different complexity levels of solution domains are shown in Figure 1-1. For different problems appropriate method should be chosen in order to get accurate and efficient solutions. For example in an aircraft flutter problem highly non-linear fluid domain should be modeled using Euler or Navier-Stokes equations. But in simpler problems using these equations may increase solution time unnecessarily. Also in a biomechanics problem such as modeling aortic

valve, detailed 3D finite element solution can be used to model the complex geometry. However a simple flat plate can be modeled using a simpler technique. When the decision on the fluid and structure domain solution method is done, the FSI problem can be solved using three major approaches that are fully coupled, closely coupled and loosely coupled approaches.

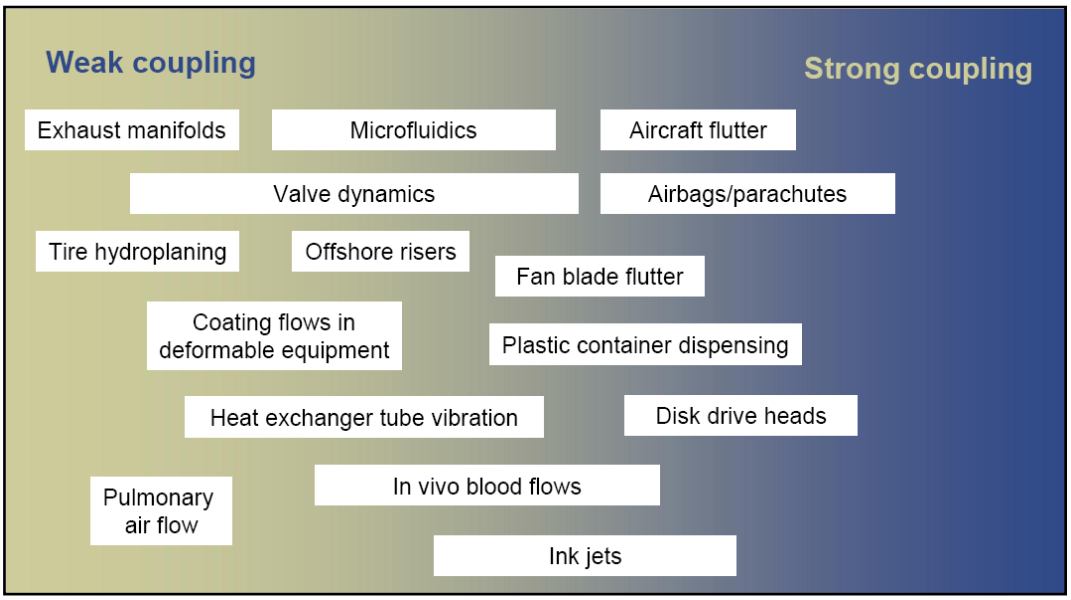

Figure 1-2 Coupling interface complexity for different problems [3]

1.1 Coupling Approaches

Independent from the complexity of the fluid solution or structural solution, different problems work best with different coupling methods. In Figure 1-2 FSI problems are listed according to the complexity of their coupling interface, that is complexity of physics how the fluid and structural parts of problems affected by this interface. It must be noted that this figure does not show the complexity of the solution in the fluid or structural domain.

Development of numerical solution techniques to complex fluid structure interaction problems with acceptable efficiency and accuracy is an active research topic. The idea is to model time dependent non-linear fluid flow by using Euler or Navier-

Stokes equations and couple these models with elastic structures which can be either linear or nonlinear. The problem can be modeled using fully coupled methods (simultaneous) like Kroyer's studies [1], loosely (weak) coupled methods as in the Sümer's solution of aircraft wing [10] or closely (strong) coupled methods as described in Başkut's thesis studies [11].

1.1.1 Fully Coupled Approach

In fully coupled solutions, structural and fluid equations of motion are combined into a single set of governing equations which are solved in a single iteration loop simultaneously in order to get accelerated convergence rates and more stable solutions. Besides these advantages, structural and fluid equations, being on a Lagrangian and an Eulerian system respectively, must be solved together in a fully coupled solver, which brings computational difficulties during the solution process [4]. Also in fully coupled solution procedures same time discretization scheme is used for all subsystems which may be inefficient. Moreover a new development of a completely new solver is required and parallel computing is difficult for fully coupled solution procedures [3].

1.1.2 Closely Coupled Approach

In closely coupled approach, structural and fluid equations are solved separately using two different codes and two solution domains. Usually these two computational domains (grids) do not coincide, which results with the need for a method to transfer information from one to another. The information obtained from each solver is interchanged between the codes. The major aspect of closely coupled approach different from loosely coupled approach is the coverage of each time step after the convergence of an additional inner fluid-structure loop. Separate solvers undergo an additional iteration loop for each time step which makes the solution more stable and gives better convergence behavior. However more numerical effort should be performed for close coupling algorithms. Thanks to this aspect of closely

coupled approach, complex and non-linear FSI problems can be solved using this method [4].

1.1.3 Loosely Coupled Approach

In loosely coupled approach, two different solvers which use different computational grids are used for the solution of fluid and structure problems. Also in loosely coupled approach these two computational domains (grids) do not coincide, which results with the need for a method to transfer information from one to another. Information from one solver is transferred to other solver after the convergence. As a result main challenge of this approach is to develop a coupling procedure. In loosely coupled approach one has the possibility to choose any fluid or structural solver and apply a coupling procedure to solve the problem, which is the major advantage of this approach. One disadvantage of loose coupling is the reduced accuracy since information transfer takes places only at each time step, so it is applicable to problems having rather less complexity and non-linearity [4]. In this thesis loosely coupled approach is chosen due to its flexibility and requirements of less computational power. A table comparing closely and loosely coupled approaches is given Table 1-1.

Table 1-1 Comparison of Closely and Loosely Coupled Approaches [3]

	Close Coupling	Loose Coupling
Convergence Behavior	✓	×
Stability	✓	×
Numerical Effort	×	✓
Available Technology	×	✓
Computation Time	✓	×
Hardware Requirement	×	✓

1.2 Aeroelastic Problems in Missiles and Rockets

The main area of research of aeroelasticity has been the airplane wings. Due to their low weight, high flexibility, high load and high safety requirements, airplane wings are usually designed at limits, which may result in aeroelastic problems. As a result aeroelastic analysis is an important step in airplane design. However in the design of a missile or a rocket, aeroelastic effects are rarely taken into account. But in real life, due to aeroelastic effects following situations may occur for missiles or rockets:

- High aerodynamic forces may result in the mechanical failure of control surface(s) or stability fin(s), thus aerodynamic control of the missile may be lost.
- Deformations in the control surfaces or stability fins may reduce the lift force produced by these fin sets. Also reduced lift force in the control surfaces may result in reduced control effectiveness and maneuverability. Moreover stability characteristics of the missile may also change due to deformations.
- Deformations in the control surfaces may also change the center of pressure location at the fin which may cause high hinge moments around hinge lines. Thus enough power may not be produced to control the missile aerodynamically.
- Vibrations that occur due to aeroelastic effects may affect the avionics of the missile. Sensors used in inertial measurement unit may be affected by these vibrations which would result in increased error in the flight computer calculations and trajectory. Also guidance systems of the missile may be affected from these vibrations that may reduce the hit probability and accuracy of the missile.

To overcome the problems described above, aeroelastic analysis should take place in the design of missiles and rockets. For different problems and situations, static and/or dynamic aeroelastic calculations, simulations and tests may be conducted.

1.3 Literature Survey

Previous studies mostly cover development of solution techniques for the solution of aeroelastic problems such as wing flutter analysis. Lui et al. developed a method for simulation and prediction of wing flutter problems by integrating CFD and CSD tools [5]. Euler and Navier-Stokes equations are modeled by a CFD solver which is an unsteady, parallel, multi-block, multi-grid finite volume solver. CSD solver extracts modal equations and integrates over time. Both solutions are implicitly coupled with a strong coupling algorithm. A two dimensional and a three dimensional AGARD 445.6 wing are used for computations and the results are compared with experiments.

Kamakoti and Shyy investigated models for interaction problems for different applications and developed an efficient coupling interface [4]. Also they covered the recent advancements in FSI field. Several techniques are reviewed to develop a robust coupled aeroelastic model. Wing flutter calculations at different Mach numbers are conducted for AGARD 445.6 wing. Slone et al. developed an approach which handles three fields: fluid flow, structural dynamics and mesh movement [6]. This strategy makes calculations using a single mesh for both domains, a Navier-Stokes flow solver with finite volume and unstructured mesh discretization and Newmark algorithm. These features are brought together in a single program. They modeled a three dimensional cantilever beam in fluid flow to demonstrate basic wing dynamic characteristics. Kroyer performed analyses of a 2D wing profile by using the fully coupled FSI simulation software ADINA [1]. Steady state and frequency domain analyses were made under flow conditions up to Mach 2. Lesoinne et al. developed a linearized method to perform aeroelastic simulations in subsonic, transonic and supersonic flow regimes [7]. They validated their method by simulating AGARD 445.6 wing. Zwaan and Prananta developed a method to analyze transonic aeroelastic effects on aircrafts by coupling the structural model with Euler or Navier-Stokes solver [8]. They used several test cases in their study. Cai et al. developed an integrated scheme using CFD and CSD methods [9]. Fluid domain

solver can handle both Euler and Navier-Stokes equations. They studied static aeroelastic calculations using AGARD 445.6 wing.

Besides the studies about FSI and aeroelasticity from all around the world, some studies were also conducted in Turkey too. Sümer developed a method to solve static aeroelastic problems concerning aircraft wings [10]. Fluid motion solver is a 3D Euler solver which is coupled with a commercial structural solver using a loosely coupled approach. He also used a finite element method based mesh deformation algorithm. Başkut performed closely coupled aeroelastic analysis for static and dynamic problems [11]. Frequency domain analysis was conducted and AGARD 445.6 wing was used to validate the method.

1.4 Aim of the Thesis

The aim of this thesis is to develop a loosely coupled fluid-structure interaction analysis method for the solution of static missile/rocket aeroelastic problems. FLUENT will be used as the CFD solver whereas ANSYS Mechanical will handle the structural problem. The method will be validated using AGARD 445.6 wing [12] and the results will be compared with a reference study [9]. After validating the method, static aeroelastic effects on a generic slender missile/rocket configuration will be investigated.

CHAPTER 2

METHODOLOGY

Methodology used in the calculations of the numerical simulation is described in this chapter. Governing equations related to fluid flow and structural dynamics will be given first. After the description of governing equations, numerical tools used in the analyses will be explained. Finally the numerical simulation procedure used in this study will be discussed.

2.1 Governing Equations

2.1.1 Fluid Dynamics

Numerical simulation of an aeroelastic problem is an expensive process which requires a large amount of computational hardware and long time. In order to reduce these requirements, one must make some assumptions in the solution methods. In aerospace applications, where viscous forces are dominated by inertial forces due to high Reynolds number flow conditions, neglecting viscous effects may be appropriate. Invicid flow assumption results in easier coupling calculations, since there would be no need for any boundary layer grid in the fluid domain. Details about this issue will be given later.

In invicid flows, Euler equations are solved which covers conservation of mass, momentum and energy as given below:

$$\frac{\partial \rho}{\partial t} + \nabla \bullet \left(\rho \vec{V}\right) = 0 \tag{2.1}$$

$$\frac{\partial}{\partial t}\left(\rho \vec{V}\right) + \nabla \bullet \left(\vec{V} \otimes \left(\rho \vec{V}\right)\right) + \nabla p = 0 \tag{2.2}$$

$$\frac{\partial E}{\partial t} + \nabla \bullet \left(\vec{V}\left(E + p\right)\right) = 0 \tag{2.3}$$

where ρ is the density, $\vec{V}$ is the velocity vector, E is the internal energy and p is the pressure. In addition to Euler equations, the following ideal gas relation must be used

$$\rho = \frac{p}{\frac{R}{M_\omega} T} \tag{2.4}$$

where R is the universal gas constant, M_w is the molecular weight of the fluid and T is the temperature. To characterize the compressible flow, stagnation state properties should also be calculated. Total temperature T_0 and total pressure p_0 are related to static temperature and static pressure as follows [14]

$$\frac{p_0}{p} = \left(1 + \frac{k-1}{2} M^2\right)^{\frac{k}{k-1}} \tag{2.5}$$

$$\frac{T_0}{T} = 1 + \frac{k-1}{2} M^2 \tag{2.6}$$

2.1.2 Structural Dynamics

In this part principles and governing equations concerning structural dynamics will be discussed. Stress strain relationship for a linear material is given as follows

$$\{\sigma\} = [D]\{\varepsilon\} \tag{2.7}$$

where $\{\sigma\}$ is the stress tensor, $[D]$ is the elasticity matrix and $\{\varepsilon\}$ is the strain vector. Sign convention for stress vector is given in Figure 2-1.

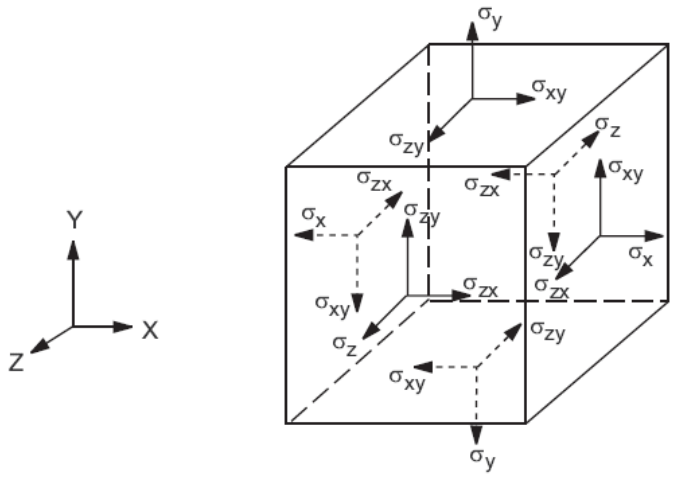

Figure 2-1 Stress Vector and Sign Convention

Also elasticity matrix can be written as

$$[D]^{-1} = \begin{bmatrix} 1/E_x & -\upsilon_{xy}/E_x & -\upsilon_{xz}/E_x & 0 & 0 & 0 \\ -\upsilon_{yx}/E_y & 1/E_y & -\upsilon_{yz}/E_y & 0 & 0 & 0 \\ -\upsilon_{zx}/E_z & -\upsilon_{zy}/E_z & 1/E_z & 0 & 0 & 0 \\ 0 & 0 & 0 & 1/G_{xy} & 0 & 0 \\ 0 & 0 & 0 & 0 & 1/G_{yz} & 0 \\ 0 & 0 & 0 & 0 & 0 & 1/G_{xz} \end{bmatrix} \tag{2.8}$$

where E_i is the Young's modulus in direction i, G_{ij} is the shear modulus in the ij-plane and υ_{ij} is the Poisson's ratio in the ij-plane. The elasticity matrix is assumed to be symmetric, yielding to the following expressions

$$\frac{\upsilon_{yx}}{E_y} = \frac{\upsilon_{xy}}{E_x}$$
$$\frac{\upsilon_{zx}}{E_z} = \frac{\upsilon_{xz}}{E_x} \qquad (2.9)$$
$$\frac{\upsilon_{zy}}{E_z} = \frac{\upsilon_{yz}}{E_y}$$

For an isotropic material shear modulus can be calculated as

$$G_{xy} = G_{yz} = G_{xz} = \frac{E_x}{2\left(1+\upsilon_{xy}\right)} \qquad (2.10)$$

When Equation (2.7) is rearranged using above expressions the following six equations can be obtained.

$$\varepsilon_x = \frac{\sigma_x}{E_x} - \frac{\upsilon_{xy}\sigma_y}{E_x} - \frac{\upsilon_{xz}\sigma_z}{E_x}$$
$$\varepsilon_y = -\frac{\upsilon_{xy}}{E_x} + \frac{\sigma_y}{E_y} - \frac{\upsilon_{yz}\sigma_z}{E_y}$$
$$\varepsilon_z = -\frac{\upsilon_{xz}\sigma_x}{E_x} - \frac{\upsilon_{yz}\sigma_y}{E_y} + \frac{\sigma_z}{E_z} \qquad (2.11)$$
$$\varepsilon_{xy} = \frac{\sigma_{xy}}{G_{xy}}$$
$$\varepsilon_{yz} = \frac{\sigma_{yz}}{G_{yz}}$$
$$\varepsilon_{xz} = \frac{\sigma_{xz}}{G_{xz}}$$

2.2 Numerical Tools and Numerical Simulation Methodology

As described in the previous chapter, in loosely coupled approach one has the flexibility of choosing separate flow and structural solvers. In this part flow and

structural solvers, mesh deformation technique and data transfer methodology used in this study will be covered.

2.2.1 Computational Fluid Dynamics Solver

When the governing equations for fluid motion are examined, it is obvious that these equations are nonlinear and for very limited problems exact solutions can be obtained [16]. For problems including rather complex shapes, numerical solutions can be used to calculate a pressure distribution and hence forces and moments. In this study a commercial software FLUENT is used as the CFD solver. FLUENT is capable of solving compressible, incompressible fluid flow, heat transfer, finite rate chemistry, species transport, combustion, multiphase flow and solidification and melting problems as steady state or in time domain. FLUENT can work with a wide variety of mesh types for both 2D and 3D flow domains [17].

Tetrahedral volumes are used to discretize the 3D problem domains of this study. Solution domain for the CFD solver is generated in another commercial program GAMBIT. The grid generation procedure is simply composed of

- Import solid model to GAMBIT
- Generate surface grid using triangular elements
- Generate volume grid starting from surface grid using tetrahedral elements
- Define boundary conditions
- Export generated volume grid to FLUENT

In FLUENT scalar transport equations are converted to algebraic equations in a control volume based manner to solve the problem numerically. Transport equations are integrated over each control volume which results with an equation expressing

conservation laws. For a scalar quantity ϕ, discretized governing equations are given in the following form [13]

$$\int_V \frac{\partial \rho \phi}{\partial t} dV + \oint \rho \phi \vec{V} \bullet d\vec{A} = \oint \Gamma_\phi \nabla \phi \bullet d\vec{A} + \int_V S_\phi dV \tag{2.12}$$

where ρ is the density, $\vec{V}$ is the velocity vector, V is the volume of the control volume, A is the surface area of the control volume, Γ_ϕ is the diffusion coefficient for ϕ and S_ϕ is the source term. The above expression is the integral form of a generic conservation equation. Over the control volume this equation can be rearranged as

$$\frac{\partial \rho \phi}{\partial t} V + \sum_f^{N_{faces}} \rho_f \vec{V}_f \phi_f \bullet \vec{A}_f = \sum_f^{N_{faces}} \Gamma_\phi \nabla \phi_f \bullet \vec{A}_f + S_\phi V \tag{2.13}$$

where N_{faces} represents the number of faces of the control volume (for example for a tetrahedral element there are 4 faces) and ϕ_f is ϕ convected through face f. Illustration of such a control volume is given in Figure 2-2.

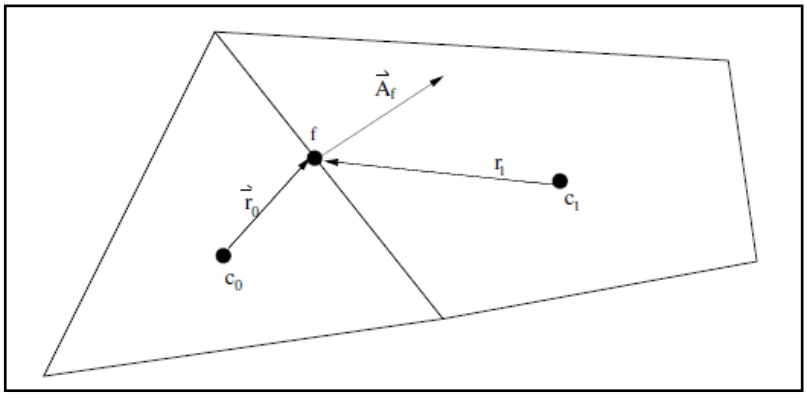

Figure 2-2 The Control Volume Used for Discretization of Transport Equation

In FLUENT two solver types are available, namely the pressure based solver and the density based solver. Pressure based solver is initially developed for low speed

incompressible flows, whereas density based solver is developed for high speed compressible fluid flow. Recent studies and developments made it possible to use both solver types in a wide range of flow regimes and conditions [13].

The pressure based solver uses a type of projection method in which the pressure equation is rearranged from momentum and continuity equations [18]. Two different algorithms, known as segregated and coupled, can be used in FLUENT. In segregated algorithm the governing equations are solved sequentially and iteratively in a loop to obtain converged solutions. Segregated solver needs less memory but relatively more time for the problem solution. In coupled solver governing equations are solved together as a single set of equations. For this reason memory requirements increase whereas time requirements for convergence decrease dramatically [13]. In this study governing equations, which are momentum, continuity and energy equations are solved simultaneously using the density based solver. To obtain a converged solution an iterative procedure should be followed since the equations are nonlinear.

In density based solver, the governing equations can be solved either by explicit or implicit formulation. In implicit formulation, for a solution of a variable both known and unknown variables are used in the formulation. But in explicit formulation only known variables are used for the solution of the desired variable. To conclude all the variables in all cells are solved together in coupled implicit solver. All the variables in one cell are solved together in coupled explicit solver [13].

For CFD simulations used in this thesis, pressure based segregated solver will be used for subsonic speeds whereas density based implicit solver will be used for supersonic speed simulations due to convergence problems faced when pressure based segregated solvers are used for supersonic invicid problems. In the CFD simulations that will be performed in this thesis, as convergence criteria the last 100 iteration steps will be investigated to see whether the percent difference of lift

coefficient between first and last steps are less than 1 %. When this criterion is achieved, simulation will be considered to be converged.

2.2.2 Computational Structure Dynamics Solver

As the computational structure dynamics solver ANSYS will be employed. ANSYS is capable of solving steady state problems containing external pressures and forces, steady state inertial forces, imposed displacements, temperatures and fluencies Calculations for steady loading conditions in which effects of damping and inertia are ignored will be conducted in this study [19].

Since the problems that will be simulated in this study do not contain any non-linearities such as large deformations or plasticity, linear static analysis option of ANSYS is applicable. For linear static structural analyses two element types shown in Figure 2-3 are used in the simulations depending on the problem complexity. The first element type is an 8 node brick element (SOLID185) which is used for wings. For a missile, which has a more detailed body geometry, mapped or swept 8 node brick elements cannot be used. For that reason 4 node tetrahedral elements are used with free meshing approach. Elements having mid-nodes usually give better results. However elements having mid-nodes cannot be handled in the mesh deformation process. So the use of elements having mid-nodes is left as a future work.

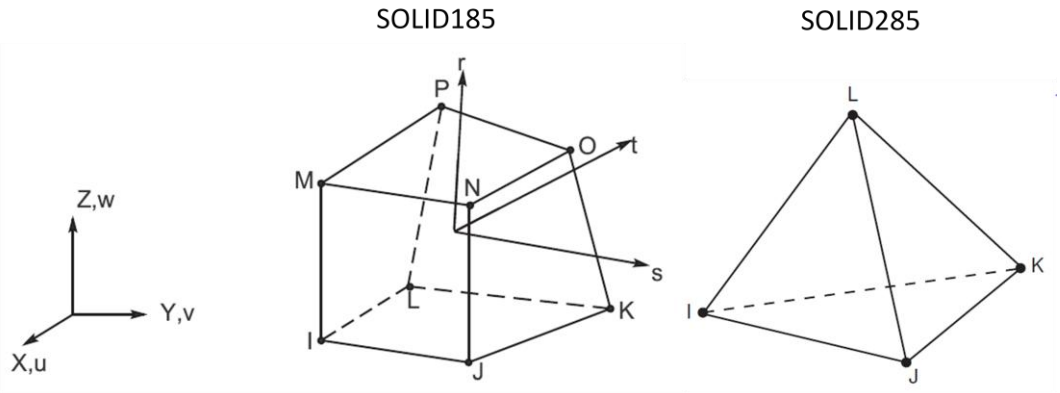

Figure 2-3 ANSYS SOLID185 and SOLID285 Elements

Simulation procedure in ANSYS can be described as the follows [19]

- The model is built first by forming the problem geometry, defining element type and preparing the grid
- Solution controls are set according to linear modeling options
- Structural loads and limitations are determined
- Solution of the problem and postprocessing is done

The problem geometry is imported to ANSYS in *"parasolid"* format which is created in GAMBIT before. After the element type is selected, grid is prepared by the built-in mesh generator of ANSYS. After setting structural limitations the database that contains grid, material properties and solution preferences is saved in an appropriate folder in the computer. An ANSYS Parametric Design Language (APDL) script is written that calls the database saved before. After the database is opened the script reads the load data which was previously generated using CFD data. This script solves and extracts nodal displacements to another file which will be processed later.

2.2.3 Mesh Deformation Methodology

Solution of a FSI problem requires deformation of fluid domain due to displacement of the geometry. In this study, spring based smoothing method present in FLUENT is used for the mesh deformation process. Displacements of the fluid domain nodes obtained by ANSYS structural solver are read by a user defined function (UDF) written in C language and compiled in FLUENT. Displacement values are then added to current node coordinates and new node coordinates are obtained. Using the spring based smoothing method, grid quality is granted by distributing the deformation all over the fluid flow domain.

In spring based smoothing method a network of springs is formed by idealizing the edges between mesh nodes as springs. Any change in the position of a node results in a new equilibrium position of the spring network and hence deforming the mesh. Force on node i can be calculated using Hook's law as [13]

$$\vec{F}_i = \sum_{j}^{n_i} k_{ij}\left(\Delta\vec{x}_j - \Delta\vec{x}_i\right) \tag{2.14}$$

where $\Delta\vec{x}_i$ and $\Delta\vec{x}_j$ are node displacements, k_{ij} is the spring constant between node i and a neighboring node j and n_i is the number of neighbor nodes. Spring constant can be written as

$$k_{ij} = \frac{1}{\sqrt{\left|\vec{x}_i - \vec{x}_j\right|}} \tag{2.15}$$

Spring constant can be selected in the range 0 to 1. The closer the spring constant to 0, the further nodes are affected by the displacement of surface nodes whereas the closer the spring constant to 1, only the mesh nodes near the deformation zone is affected by the surface displacement. To satisfy equilibrium condition, calculated force on a node should be zero. Also known deformations at the boundaries make it possible to calculate equilibrium node displacements iteratively. In the following figure an illustration is given showing initial and final positions of a deforming cylinder using spring based smoothing.

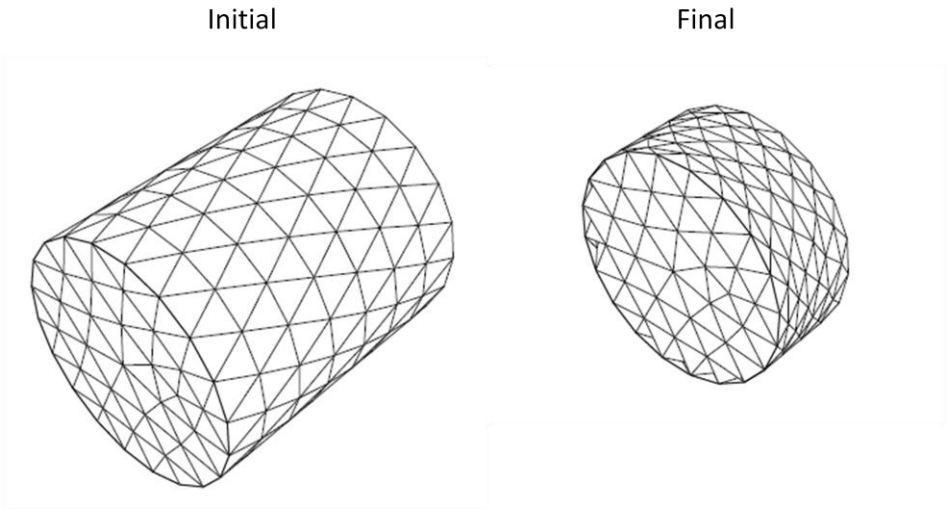

Figure 2-4 Deforming Cylinder Using Spring Based Smoothing Method [13]

2.2.4 Data Transfer Between Fluid and Solid Meshes

In the solution of a fluid structure interaction problem where loosely coupled approach is employed i.e. there are two separate solvers with two separate solution domains with non-coinciding nodes at the interface, a method should be developed in order to transfer data between the solvers. Such a fluid-structure interface is illustrated in Figure 2-5.

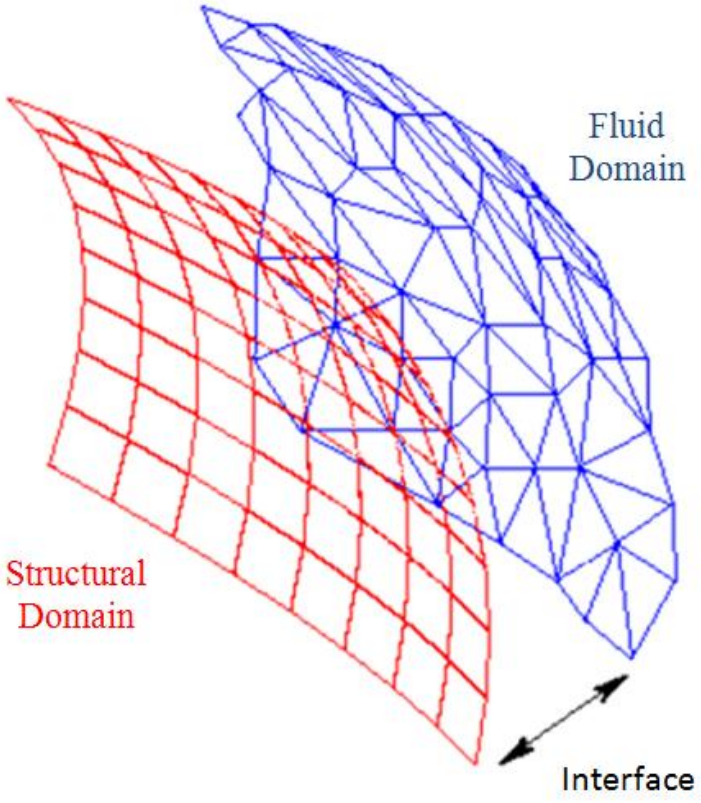

Figure 2-5 Typical Structural and Fluid Domain Interface [20]

In this thesis fluid flow domain contains high number of elements whereas in the structure domain number of elements is rather less. This results in the need of an interpolation step for data transfer between the solvers. Kriging interpolation technique will be used for data transfer with the help of TECPLOT postprocessing tool. Kriging is a complex interpolation method used for optimal prediction of random fields which gives better results than linear or inverse distance interpolation methods. Detailed description and methodology about Kriging interpolation can be

found in references [21-23]. A sample interpolation of pressure from fluid domain to structural domain for AGARD 445.6 wing is given in the following figure. As it can be seen from the contour plots, the Kriging interpolation gives highly accurate results and it is used for the entire study described in this thesis.

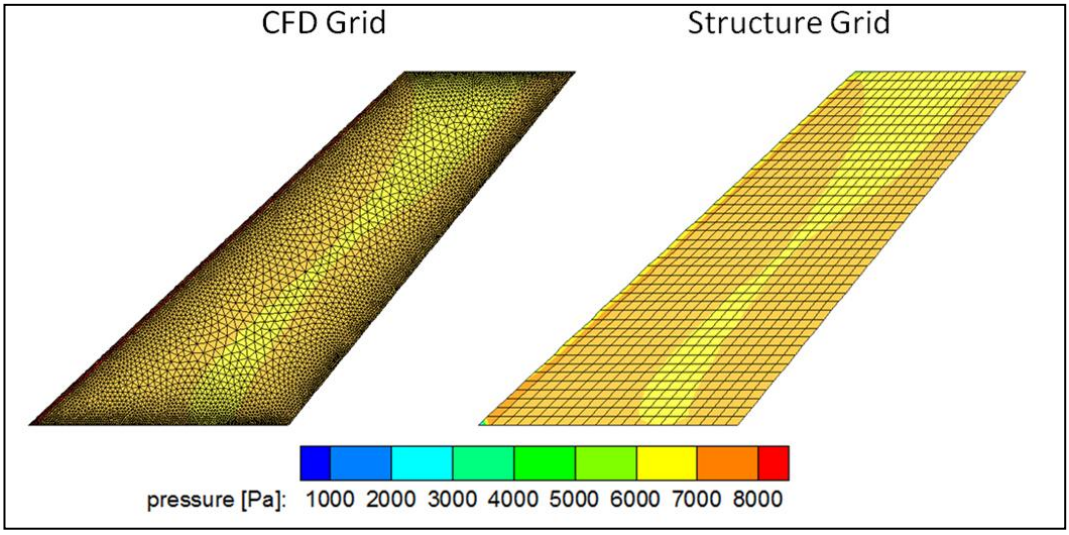

Figure 2-6 Pressure Interpolation between CFD and Structure Grids Using Kriging Technique

2.3 Steady State Fluid-Structure Interaction Simulation Procedure

Solution of a fluid-structure interaction problem requires the solution of several sub-problems such as the solution of fluid flow, solution of structural deformation, data interpolation for data transfer and mesh deformation processes. In this study these sub-problems are solved using loosely coupled approach as described in the flowchart given in Figure 2-7 and Figure 2-8.

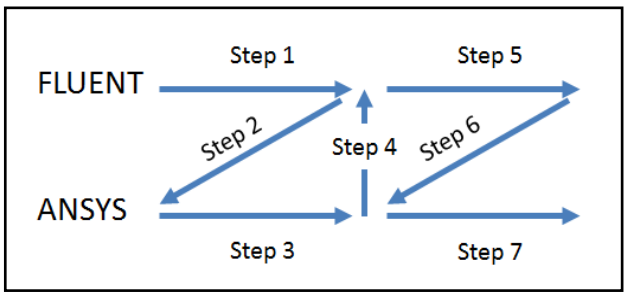

Figure 2-7 FSI Problem Solution Sequence

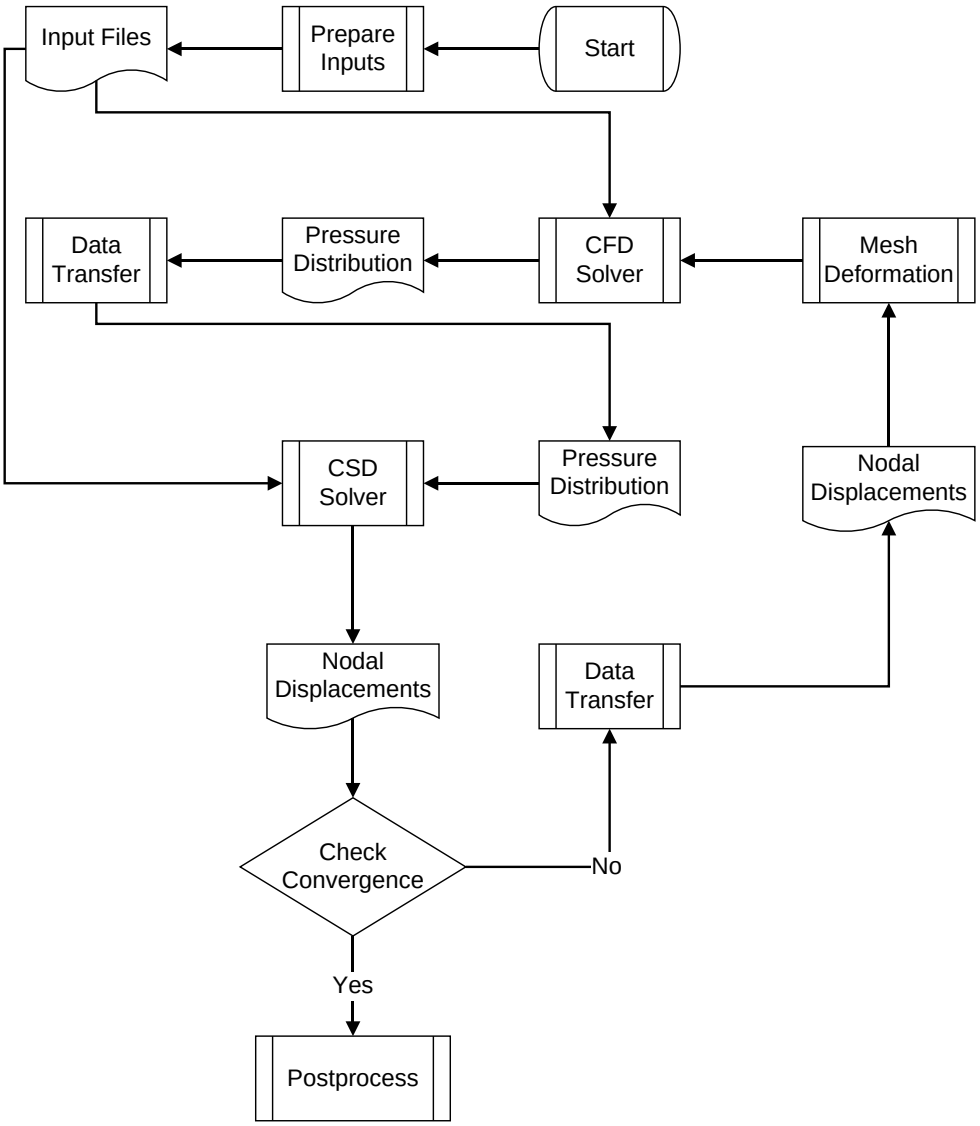

Figure 2-8 FSI Problem Solution Procedure

Solution of a fluid structure interaction problem, procedure of which is given in Figure 2-8 can be described as follows

- In order to start an analysis, first input files for fluid solver and structural solver must be prepared. For the fluid flow problem solution domain must be generated in GAMBIT and should be transferred to FLUENT. After the fluid domain is imported to FLUENT, case and data file including flight conditions

and solver types are generated. Also the user defined function that will be used for mesh deformation process is compiled for FLUENT. For the structural problem ANSYS databases and APDL script is prepared likewise.

- The first step in the FSI simulation loop is the solution of fluid flow. The case and data files generated before for rigid, steady state conditions are now ready to be solved by FLUENT. After the convergence criterion determined for FLUENT is met, solution is terminated and pressure distribution at the fluid-structure interface is exported to a file.
- Since different grids are used for structural and fluid flow problems, nodes at the interfacing boundaries do not coincide. Using the Kriging method described before, nodal pressure values are interpolated from the file exported from FLUENT in the previous step to structural grid, which is written in a separate file after the interpolation is completed.
- Previously prepared APDL script is fed into ANSYS which reads the nodal pressure values, solve the structural problem using these pressure values and write the nodal displacement values in a separate file.
- After the structural part of the problem is solved, one must decide whether the FSI simulation is converged or not. Convergence criterion can be set by the user as the maximum difference in structural displacement in the last and previous FSI iteration step.
- If convergence cannot be achieved after the solution of the structural problem, nodal displacements of structural nodes are interpolated to fluid interfacing boundary. When the interpolation is completed, FSI loop starts again from fluid flow solution with one additional process, the mesh deformation for fluid domain. This process is handled by user defined function and using spring based smoothing algorithm of FLUENT. Other steps are performed as described before.
- If convergence is achieved for FSI simulation, analysis is stopped and results can be used for postprocessing.

CHAPTER 3

TEST CASE STUDIES

Using the loosely coupled FSI method developed in this study, static aeroelastic analysis for AGARD 445.6 wing test case is conducted. AGARD 445.6 wing is a standard aeroelastic test configuration of AGARD (Advisory Group for Aerospace Research and Development of NATO) for which transonic dynamic aeroelastic tests were conducted in NASA Langley Wind Tunnel [12]. Details about this test case are given in the following section.

3.1 AGARD 445.6 Wing

As seen in Figure 3-1 aspect ratio of the wing is 1.65 and the taper ratio is 0.66. The wing has a sweep angle of 45° at quarter chord line and cross-section of the wing is NACA 65A004 airfoil in the stream-wise direction.

The test model used in wind tunnel experiments of reference [12] was constructed by laminated mahogany which is an orthotropic material with different material properties in different directions. Model used in aeroelastic tests was weakened by drilled holes which were filled by plastic foam to obtain flutter conditions easier [12]. Original AGARD 445.6 wing and weakened models are shown in Figure 3-2.

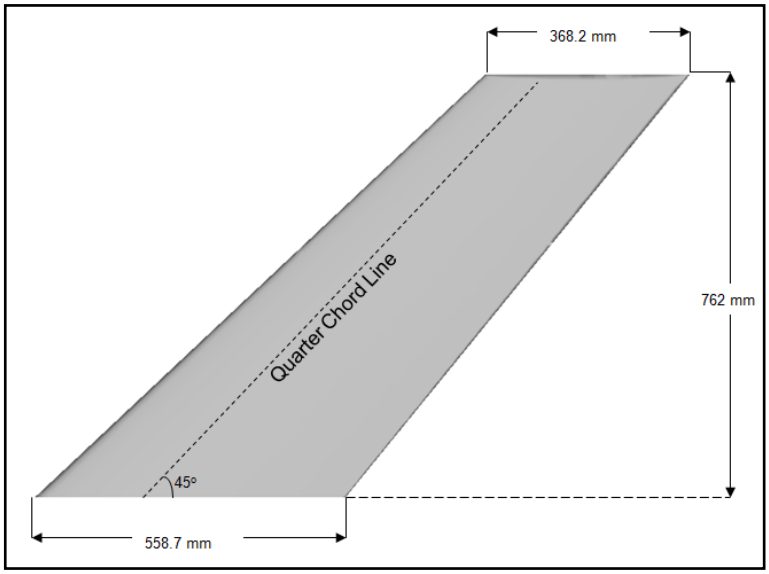

Figure 3-1 AGARD 445.6 Wing Planform Details

Table 3-1 Material Properties For Weakened AGARD 445.6 Wing [12]

Material Property	**Value [GPa]**
E_{11}	3.1511
E_{22}	0.4162
E_{33}	0.4162
G_{12}	0.4392
G_{23}	0.4392
G_{13}	0.4392
Material Property	**Value**
υ_{12}	0.31
υ_{23}	0.31
υ_{13}	0.31
Material Property	**Value [kg/m^3]**
ρ	397.5

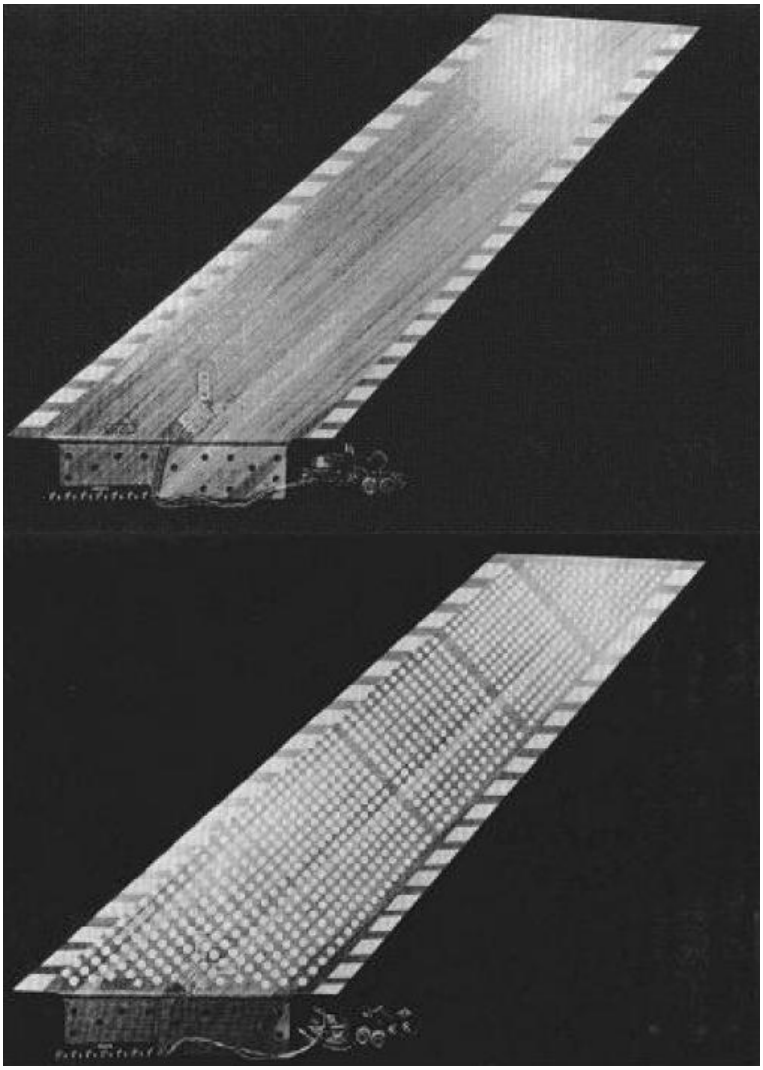

Figure 3-2 Original (Upper) and Weakened (Lower) AGARD 445.6 Wing Used for Aeroelastic Experiments [12]

Material properties for the weakened AGARD 445.6 wing can be found in Table 3-1 [12]. Fiber orientation of the weakened model is along the quarter chord line for which the properties are denoted with subscript 1. In the table E stands for modulus of elasticity, G stands for shear modulus, υ stands for Poisson's ratio and ρ stands for density.

3.1.1 CFD Grid Independency Study

In order to get results independent of grid size, one must conduct a grid sensitivity analysis. For this test case three different fluid domain grids are examined to determine the minimum allowable grid size with acceptable accuracy. Grid independency study is conducted for 0.84 free-stream Mach number and zero angle of attack. Dimensions of fluid domain are selected large enough so that boundary conditions do not affect flow over the wing. Rectangular fluid domain dimensions are given in Figure 3-3 in which dimensions are defined in chord length *c* and domain depth is 16 chord lengths.

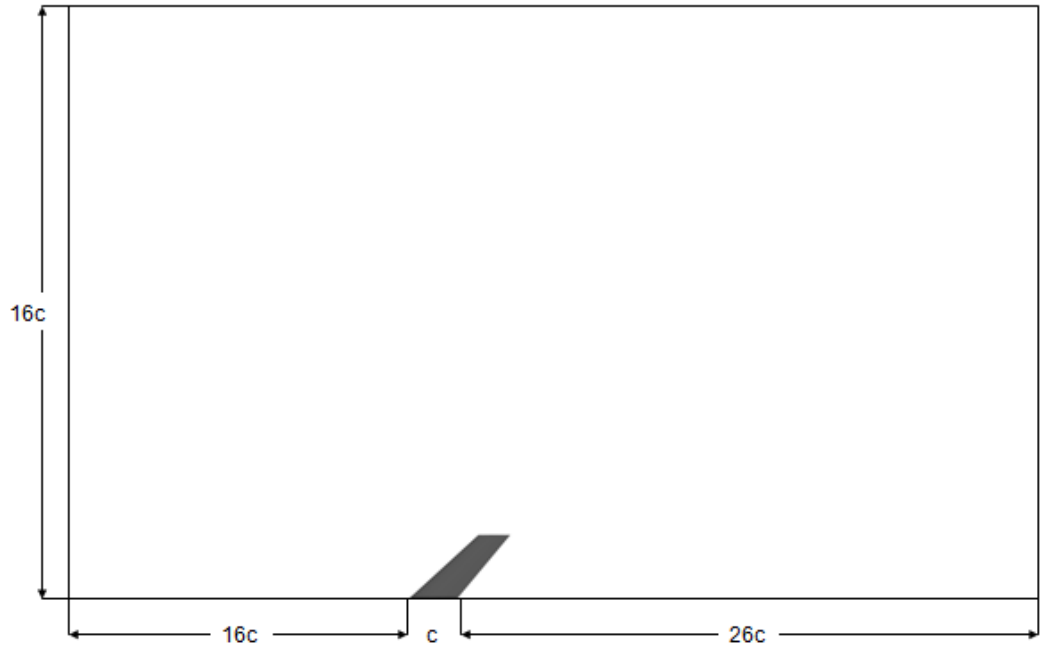

Figure 3-3 Fluid Domain Dimensions for AGARD Test Case

Boundaries of the rectangular domain that are open to fluid flow are selected as *pressure far field* boundary condition. For this boundary condition free-stream Mach number, pressure and temperature are defined according to reference [12]. Wing mounted face is defined as *symmetry* and *wall* boundary condition is used for the wing surface. Details of boundary conditions can be found in Figure 3-4. Number of elements on the wing surface and inside the whole computational domain for three

different grid configurations is given in Table 3-2. Also wing surface elements are illustrated in Figure 3-5.

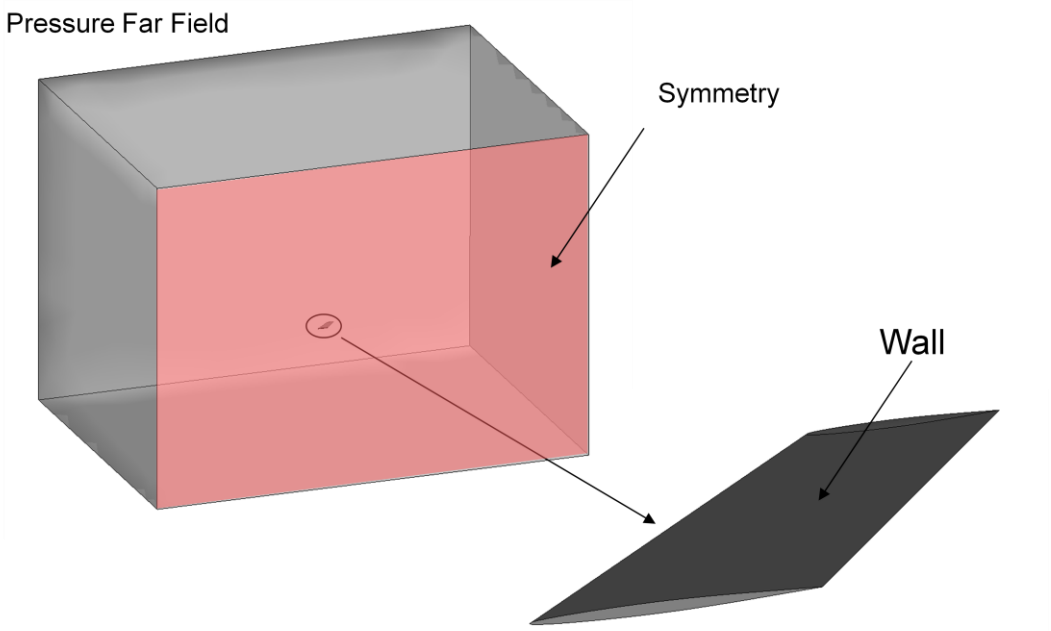

Figure 3-4 Fluid Domain Boundary Conditions

Table 3-2 Number of Elements for Different CFD Grids

Grid	Number of Elements on the Wing Surface	Total Number of Elements
Coarse	4,242	272,191
Medium	14,736	643,066
Fine	42,540	1,030,813

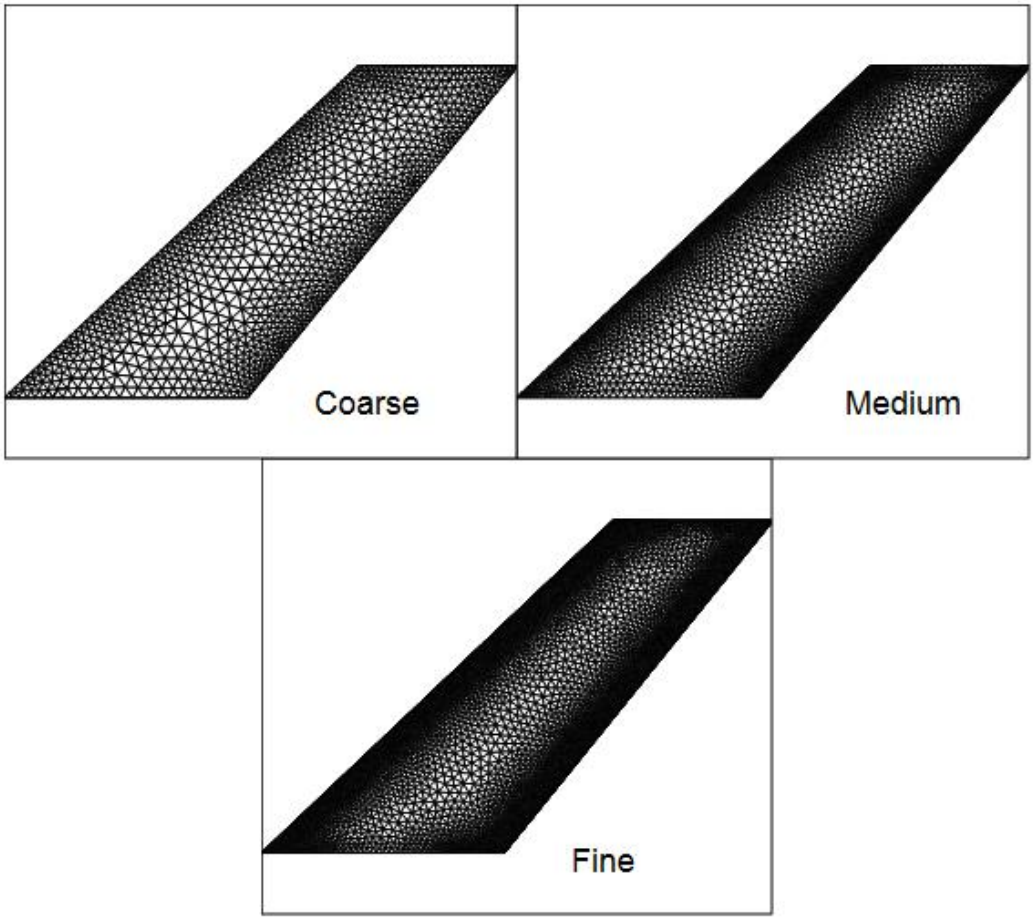

Figure 3-5 Elements on the Wing Surface for Three Different Mesh Configurations of AGARD Test Case

To determine the most appropriate grid that will be used in the static aeroelastic analysis of AGARD 445.6 wing, pressure coefficient distributions along chord-wise direction for different span locations are investigated. When Figure 3-6 is examined, it is seen that the coarse grid cannot catch the curvature of the wing and hence the pressure coefficient around the leading edge. However, medium and fine grids give close results for the entire wing. As a result medium grid is chosen to discretize the CFD flow domain for the rest of the AGARD wind simulations.

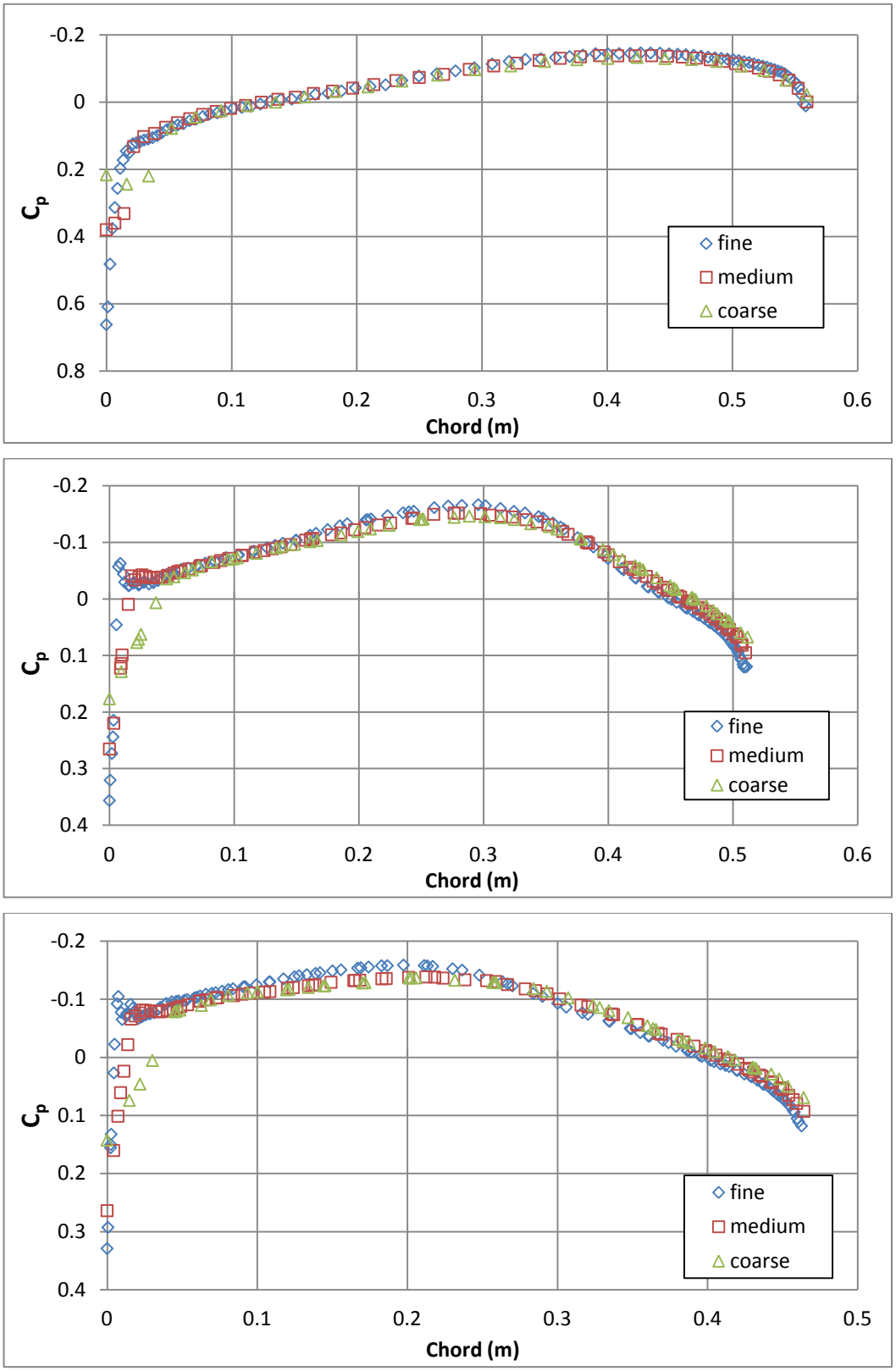

Figure 3-6 Pressure Coefficient Distribution at a) 0 % of Span b) 25 % of Span c) 50 % of Span

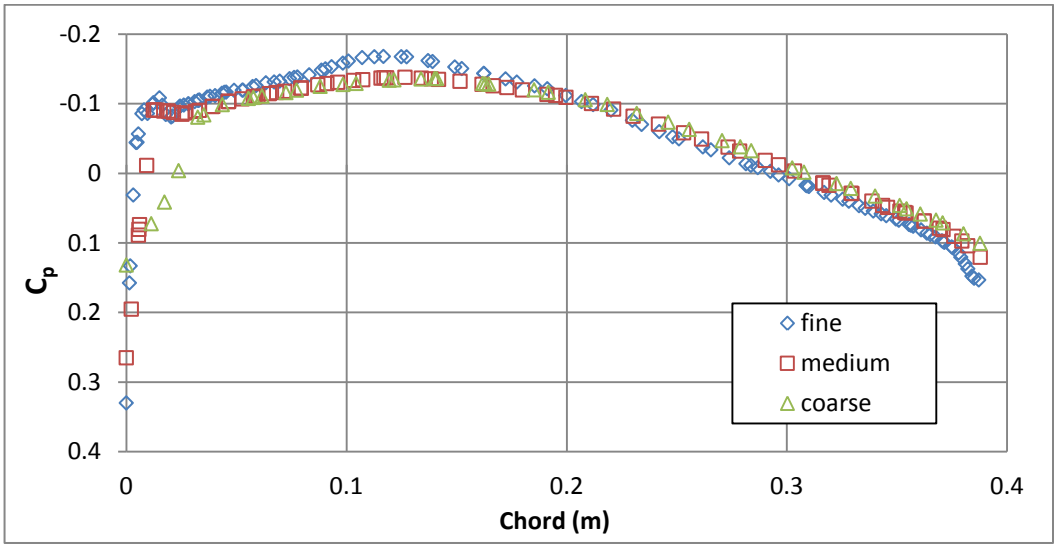

Figure 3-6(cont.) Pressure Coefficient Distribution at 90 % of Span

3.1.2 CSD Grid Independency Study

Having the similar concerns with the CFD domain, also for CSD domain a grid independency study is conducted. Three computational grids shown in Table 3-3 are generated using 8-node brick elements. Modal analyses for these grids with material properties defined in Table 3-1 are conducted to calculate first 4 natural frequencies of the wing which is at root chord. Calculated natural frequencies are compared with the experimental results given by Yates [12]. For these three grids, number of nodes and elements, calculated first four natural frequencies and comparison of these frequencies with experimental values are given in the following Table 3-4. Percent error values for these three computational domains are given in Table 3.5.

Table 3-3 Number of Elements and Nodes for Structural Grids

CSD Model	Number of Elements	Number of Nodes
Grid 1	600	1,240
Grid 2	800	1,640
Grid 3	3,500	7,100

Table 3-4 Calculated and Experimental Natural Frequency Values

Mode Number	Reference [12]	Grid 1	Grid 2	Grid 3
1	9.59	9.74	9.73	9.72
2	38.16	35.72	35.62	36.57
3	48.34	48.21	47.82	47.80
4	91.54	87.18	89.34	89.22

Table 3-5 Percent Error Values for Three CSD Grids

Mode Number	Grid 1	Grid 2	Grid 3
1	1.5	1.4	1.4
2	6.4	6.7	4.2
3	0.3	1.1	1.1
4	4.8	2.4	2.5

When the percent error values of the three computational grids are investigated, it is seen that the first mode frequency error is decreasing with the increasing number of elements. But for other frequencies one cannot outcome with a relation between number of elements and percent error. With the obtained low percent error values Grid 2 is chosen to be the structural grid for the static aeroelastic analysis of AGARD 445.6 wing.

3.2 Static Aeroelastic Analysis for AGARD 445.6 Wing

In the simulation of static aeroelastic analysis of AGARD 445.6 wing, the simulation procedure explained in Section 2.3 is followed. After the grid independency studies for CFD and CSD domains are completed, case file is prepared for FLUENT using medium grid and steady state flow simulation is conducted for the aeroelastic analysis of AGARD 445.6 wing. Flight conditions are 0.85 Mach and 5 degrees of

angle of attack. Pressure based solver is selected for the analysis and the default under-relaxation factors are decreased to increase convergence stability. Also ANSYS database file is prepared using Grid 2 and APDL script is prepared for this grid. During aeroelastic simulations nodal pressure values are interpolated from CFD grid to CSD grid and nodal displacement values are interpolated from CSD grid to CFD grid using Kriging technique using recommended settings described in TECPLOT. Previously prepared user defined function (UDF) is responsible for reading nodal displacement values for fluid domain and conduct the mesh deformation process accordingly. In the mesh deformation process, FLUENT's spring based smoothing technique is used. The spring constant is determined as 0.0001 so as to deform the mesh as homogenous as possible. Also mesh deformation process is completed at 100 steps to avoid possible negative volume occurrence in the fluid domain. As described in Section 2.3, one can use an appropriate convergence criterion to terminate the aeroelastic analysis. For AGARD 445.6 wing analysis, convergence is declared when the absolute value of the maximum deformation difference between last and previous iteration step becomes less than 1 percent of the maximum wing thickness. Currently it is not possible to run an aeroelastic analysis in a fully automated way, but instead user intervention at various steps is necessary. In this way aeroelastic analysis of AGARD 445.6 wing is completed in about 2 days. Complete automation of the method with a computer code is one of the future goals.

3.2.1 Results

In this part, results of static aeroelastic analysis for AGARD 445.6 wing are described. In Table 3-6 convergence history of the aeroelastic simulation process is given. As it can be seen, at aeroelastic iteration number 6 where the difference between last two iterations is 0.6 percent of the maximum thickness of the wing, convergence criterion described in the previous section is met and the simulation is terminated. Tabulated convergence history is also presented graphically in Figure 3-7.

Table 3-6 Convergence History of AGARD Test Case

Aeroelastic Iteration No.	Maximum Deflection [mm]	Absolute Difference Between Iterations [mm]	Percent Change
1	97.9	-	-
2	57.7	40.2	179.9
3	73.6	15.9	71.0
4	68.1	5.5	24.6
5	69.3	1.2	5.6
6	69.5	0.2	0.6

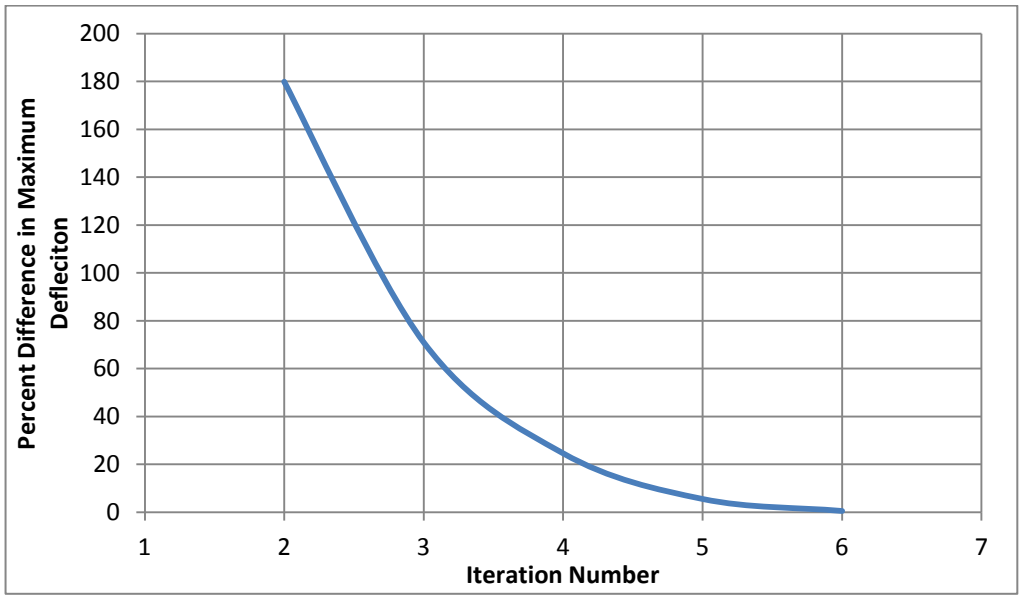

Figure 3-7 Convergence of the Aeroelastic Analysis of AGARD Test Case

In Figure 3-8 rigid wing geometry is compared with the deformed elastic wing geometry, where the maximum deflection is 69.5 mm. In Figure 3-9 a contour plot of the out of plane deformation of the wing at the end of the static aeroelastic analysis is given.

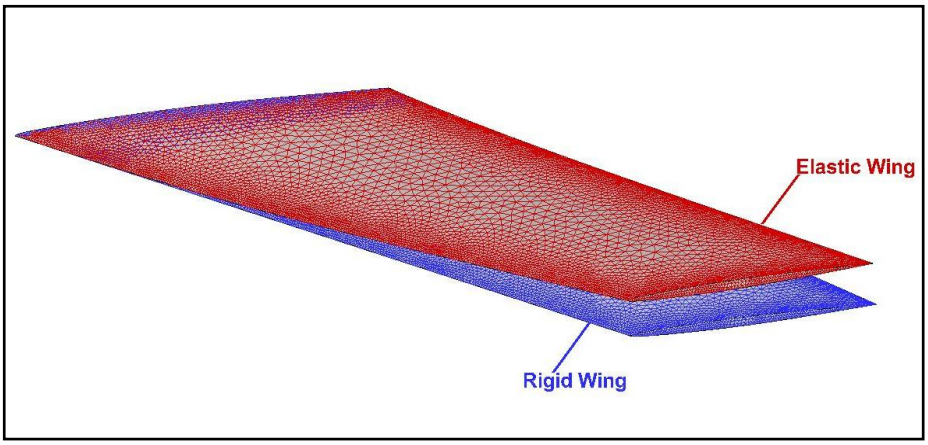

Figure 3-8 Rigid-Elastic Wing Geometry Comparison

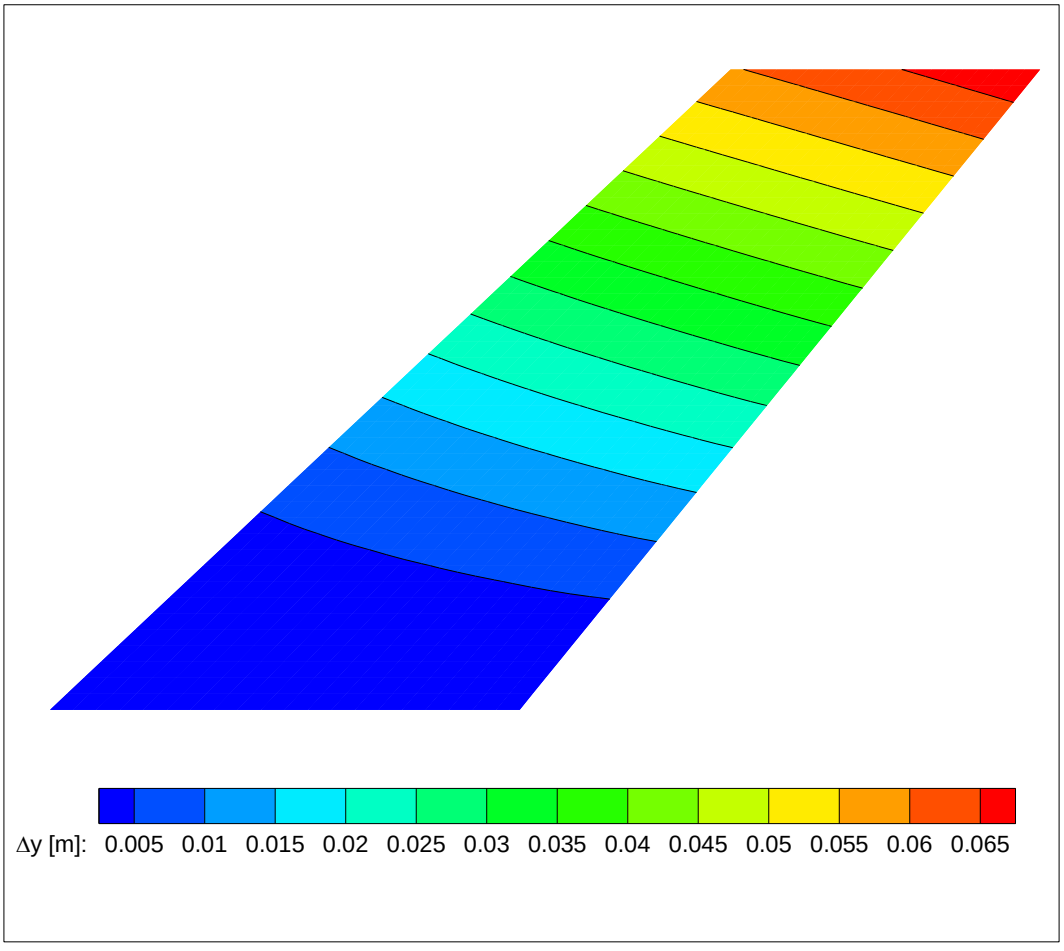

Figure 3-9 Out of Plane Deformation of Elastic AGARD 445.6 Wing

As seen from the figure the wing makes not only a y-plane motion but also a twist motion which would possibly affect the aerodynamic characteristics of the wing.
In Figure 3-10 changes of lift coefficient, leading edge tip displacement and trailing edge tip displacement during the aeroelastic iterations are presented. At the end of the aeroelastic analysis lift coefficient of the elastic wing is decreased by 19.6 percent compared with the rigid wing.

At the end of the aeroelastic analysis, tip of the leading edge deforms 5.96 cm whereas trailing edge tip deforms 6.95 cm. By using these two values approximately 1.5 degrees of twist angle can be calculated at the tip of the wing. As a result the local angle of attack at the tip of the elastic wing is 3.5 degrees whereas local angle of attack is 5 degrees for the whole wing for the rigid case. The drop in the lift force coefficient in Figure 3-10 is the result of this phenomenon.

The results of the static aeroelastic analysis conducted for AGARD 445.6 wing is also compared with the previous study of Cai et al. [9], in which Euler and Navier-Stokes based static aeroelastic analysis is present. Comparison of leading and trailing edge displacements of elastic wings are given in Figure 3-10. Both leading and trailing edge displacements are in good agreement with the reference study.

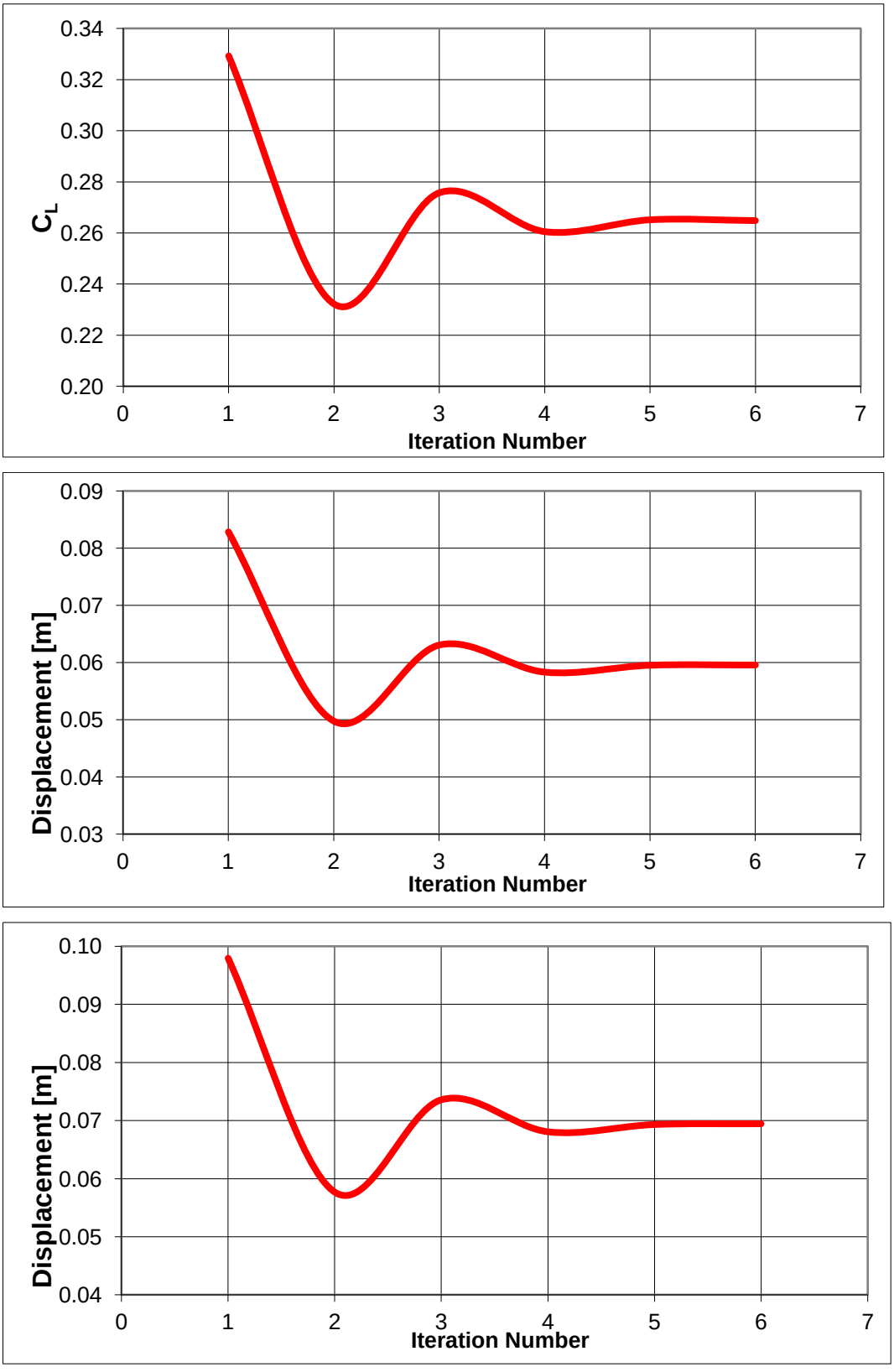

Figure 3-10 Change of Lift Force Coefficient (top), Leading Edge Tip Displacement (middle) and Trailing Edge Tip Displacement (bottom) with Aeroelastic Iteration Step

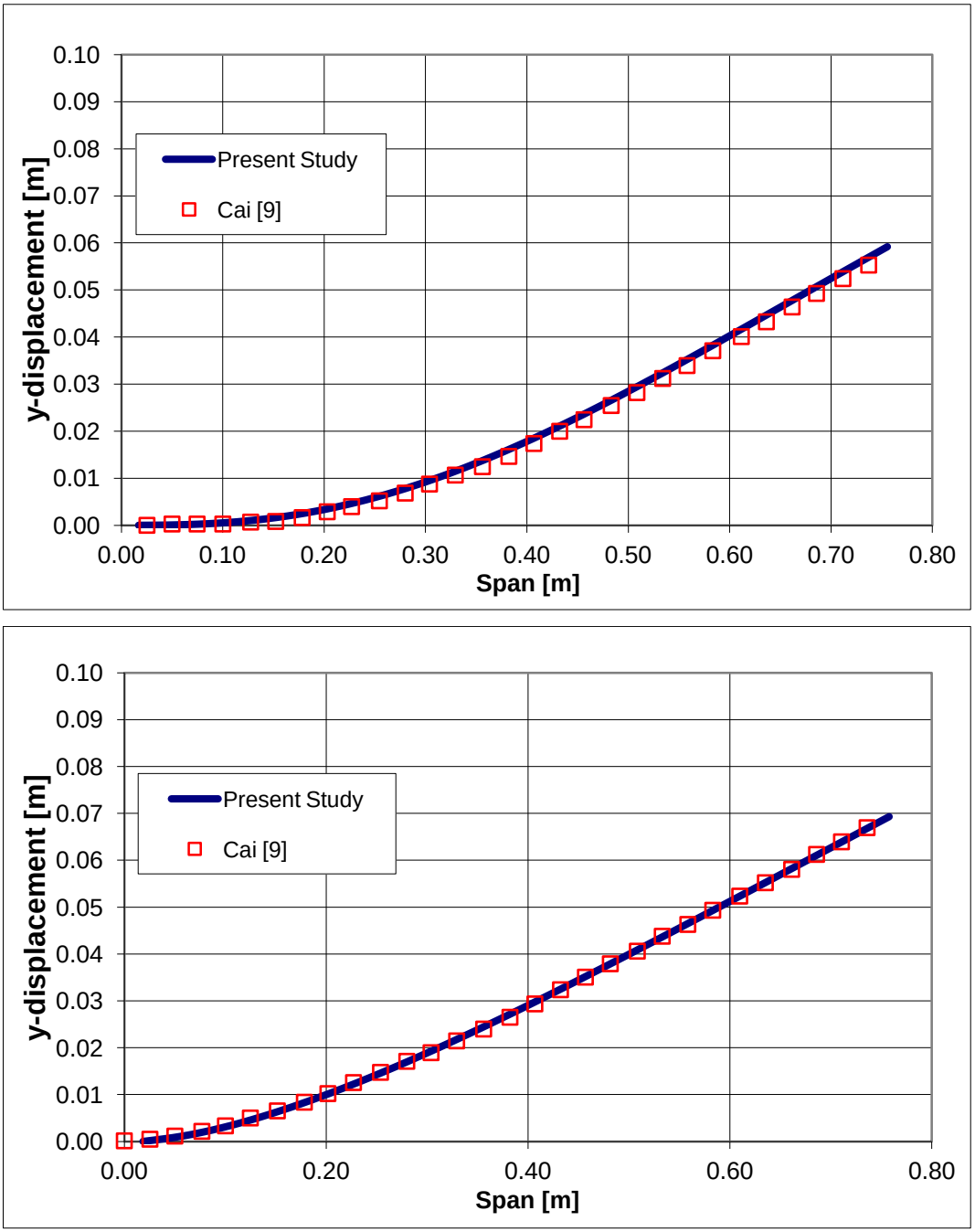

Figure 3-11 Displacement of Leading (top) and Trailing (bottom) Edges Along Wing Span

Figure 3-12 presents pressure coefficient results compared with Cai et al.'s work [9] at 34 % and 67 % of the span. Similar to the results of leading and trailing edge displacements, pressure coefficient results are also in good agreement with the reference study.

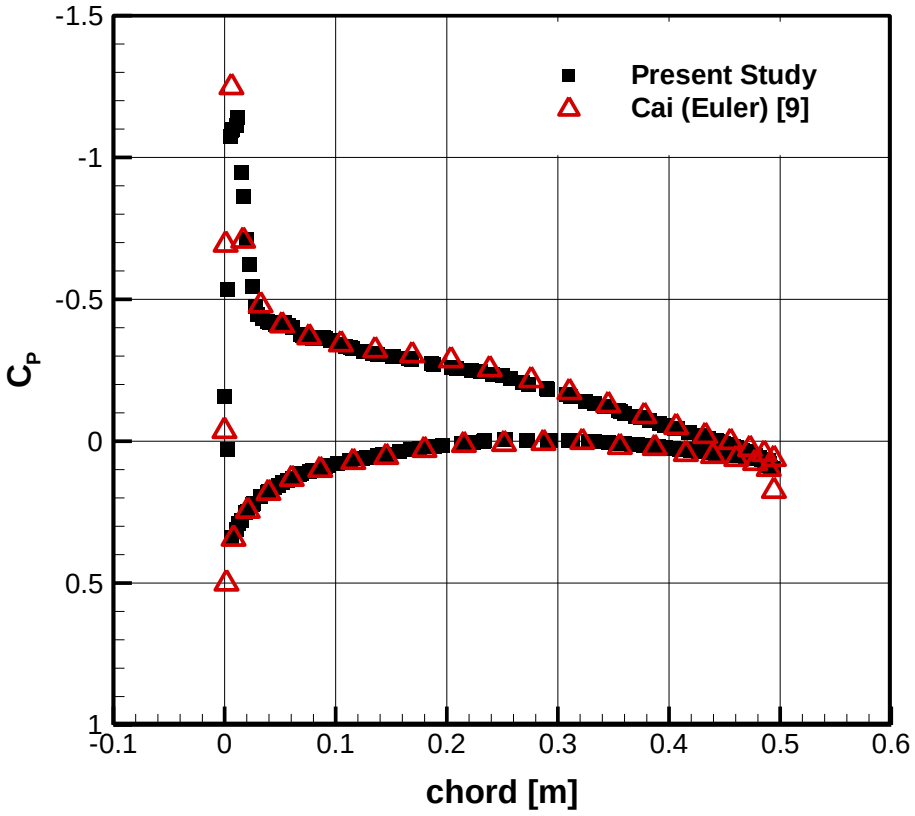

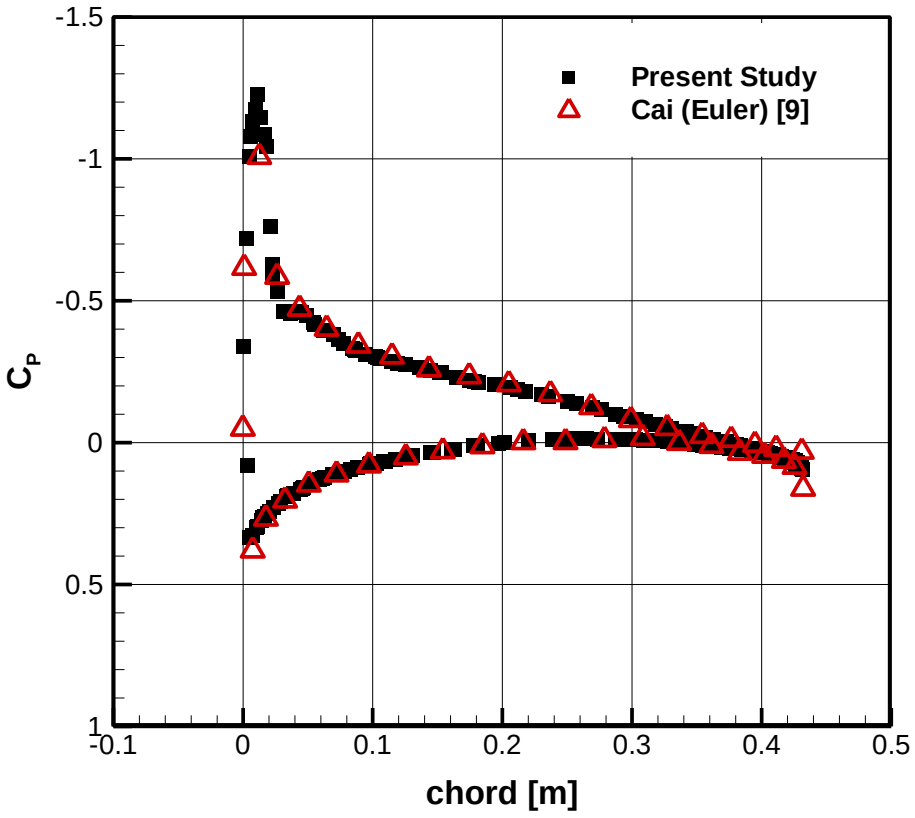

Figure 3-12 Pressure Coefficient Comparison at 34 % (top) and 67 % (bottom) of Span

3.2.2 Conclusions

In this part of the thesis, to test the loosely coupled fluid-structure interaction method developed in this study, static aeroelastic analysis are performed for AGARD 445.6 and the results are compared with reference studies.

For weakened AGARD 445.6 wing grid independency studies are conducted for both fluid and structure solution domains. After selecting the appropriate meshes, static aeroelastic calculations are conducted for flight conditions of 0.85 Mach and 5 degrees of angle of attack. Convergence is obtained at 6 iteration steps. Lift force coefficient of the wing is decreased by 19.6 % compared to the rigid wing because of the twist motion that the wing undergoes. Leading edge tip of the wing is deflected by 5.96 cm whereas trailing edge tip is deflected by 6.95 cm which leads to 1.6 degrees of twist angle. As a result of this, local angle of attack of the wing decreases along the wing span which reduces the aerodynamic performance of the wing. The static aeroelastic analysis results for weakened AGARD 445.6 wing are compared with the previous numerical studies conducted by Cai et al. [9]. Leading and trailing edge deformations and pressure coefficient are compared with their study, for which good agreement of results are obtained. Solution of this test case and the compared results shows that the developed loosely coupled fluid-structure interaction analysis method can be applicable for static aeroelastic problems.

CHAPTER 4

MISSILE AEROELASTIC STUDIES

In this part of the thesis, analysis of a generic slender missile geometry will be conducted to investigate possible static aeroelastic effects on missile like geometries. Geometry of the missile is similar to a classical 2.75" rocket geometry which has canards as control surfaces. This missile is used as a benchmark problem in ROKETSAN for aeroelastic problems. High aspect ratio of canards and highly slender missile body makes this configuration a good benchmark model to investigate aeroelastic effects on missiles. Due to privacy reasons concerning ROKETSAN, geometric details of the missile are not given in this study. Length of the missile is shown as L and moment center is taken to be at the middle of the missile which is L/2. The missile has canards as control surfaces and tails as stability fins. Tails and canards are both in + configuration. Details about the missile geometry are given in Figure 4-1 and Figure 4-2.

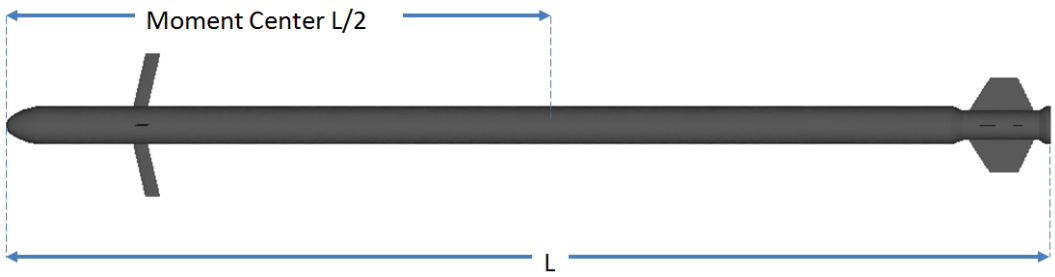

Figure 4-1 Generic Slender Missile Geometry

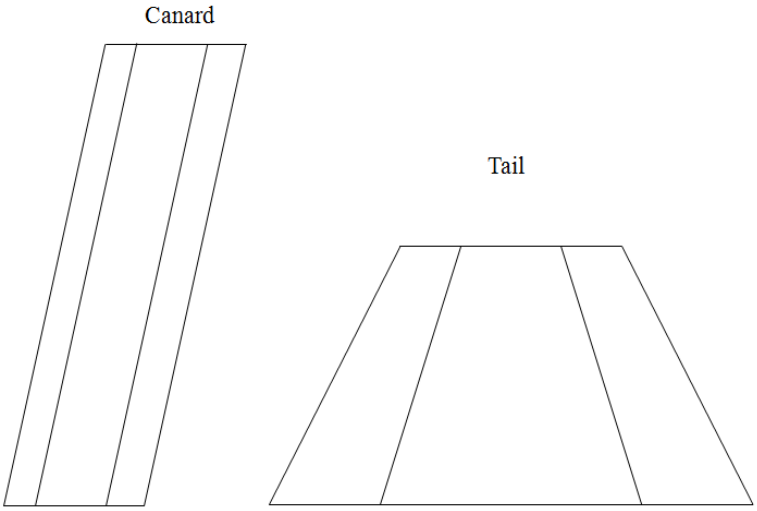

Figure 4-2 Canard and Tail Planform Geometries of the Generic Missile

Results of the aeroelastic analysis are compared with rigid missile results in order to see the possible static aeroelastic effects. Analyses for both rigid and elastic missiles are conducted for a freestream Mach number of 2 and sea level atmospheric conditions. To investigate aeroelastic effects more clearly, analyses are conducted for a critical maneuvering position, for which there is 15º canard elevator deflection angle and 10º angle of attack. Canard and tail numbering for both missiles are given in Figure 4-3. Elevator deflection is defined as canard number 2 and 4 are deflected by 15º such that leading edges of these fins move upwards.

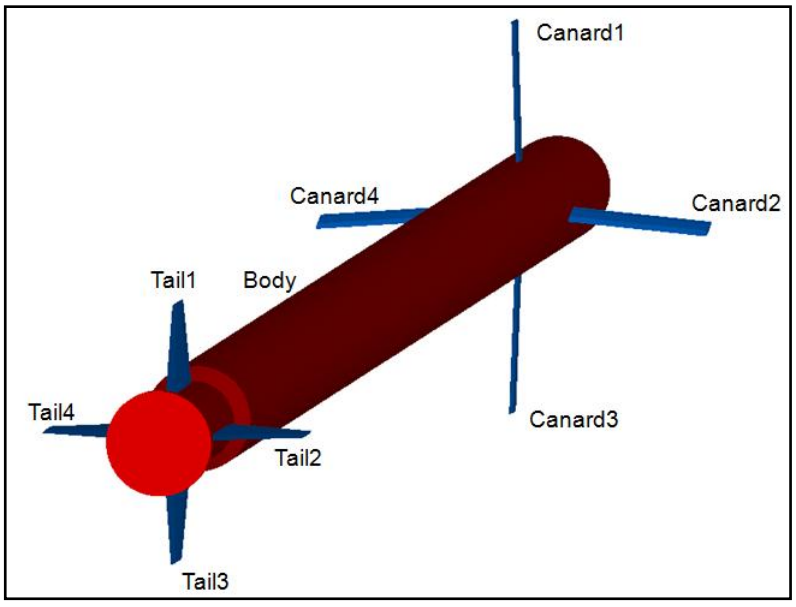

Figure 4-3 Fin Numbering for Generic Slender Missile

For rigid and elastic missile configurations same fluid domain is used for steady state analyses. Similar to previous study on AGARD 445.6 wing, fluid domain is chosen to be large enough to minimize boundary condition effects on the fluid flow over the missile. Fluid domain is selected as a cylinder and for boundary conditions all the faces of cylinder are defined as *pressure far field* whereas missile surface is selected as wall. Detail of fluid domain dimensions and boundary conditions are illustrated in Figure 4-4 and Figure 4-5.

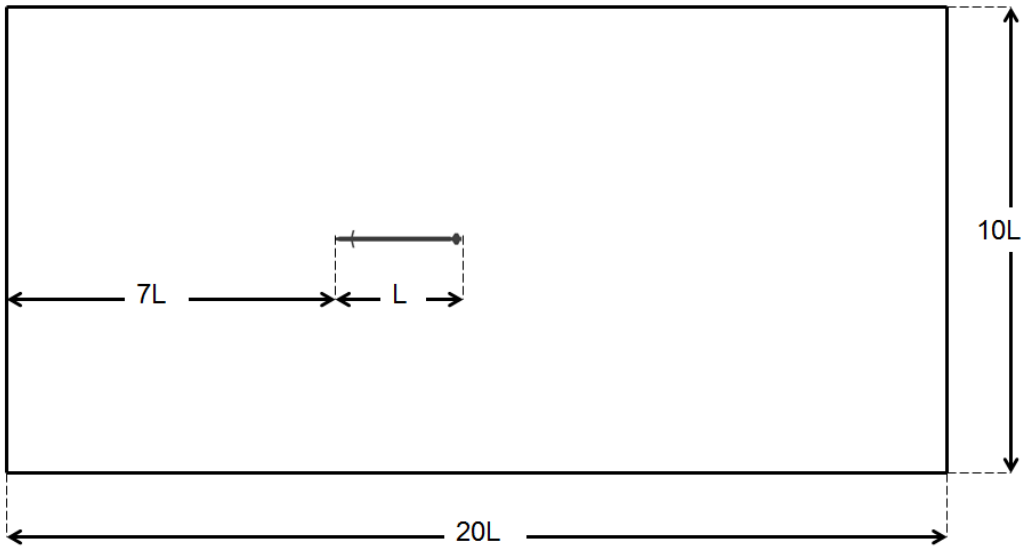

Figure 4-4 Fluid Domain Dimensions for Generic Missile

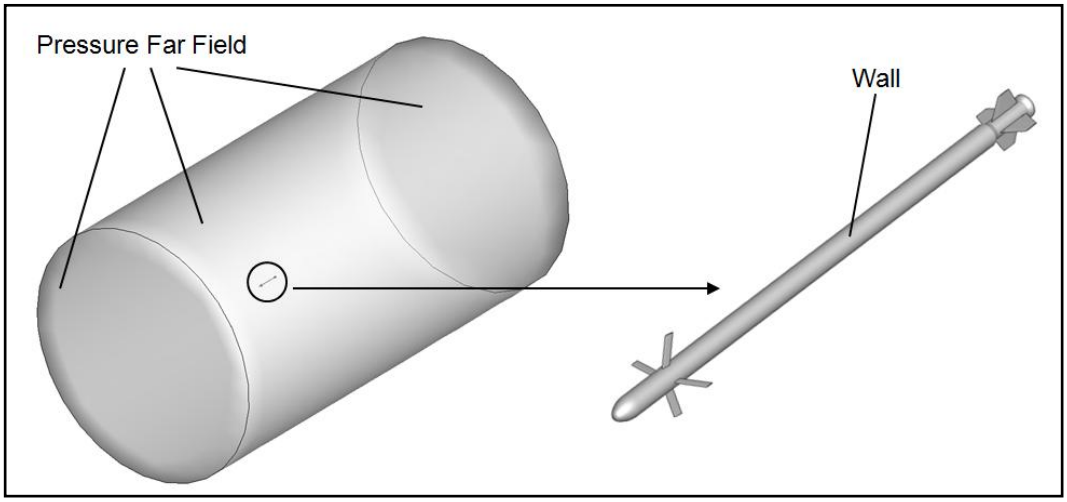

Figure 4-5 Fluid Domain Boundary Conditions for Generic Missile

Missile geometry has 41,240 triangular surface elements whereas fluid domain is composed of 3,240,611 tetrahedral volume elements which are generated in GAMBIT. An illustration about missile surface and volume grid is given in Figure 4-6.

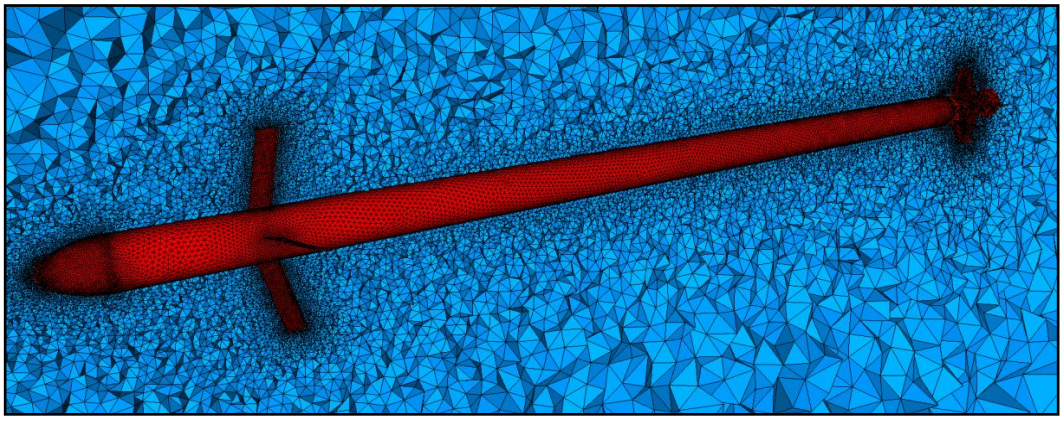

Figure 4-6 Missile Surface and Volume Grid

Similar to previous studies conducted for AGARD wing, structural model is prepared in ANSYS. For the missile geometry which is quite complex when compared to the AGARD wing, a structured-mapped grid cannot be generated using brick elements. For that reason the structural grid composed of 238,697 unstructured elements are constructed by 4 node tetrahedral elements using free meshing tool of ANSYS. Missile is translation restricted at the moment reference L/2. Canards and tails are attached to the missile body rigidly. Rigid attachment approach is a good approximation for stability fins which are tails in this study. However, control surfaces are generally connected to the missile body by shaft, which is powered by a control actuation system. In a more detailed future analysis, canards can be connected to the missile by a shaft. Body of the missile is modeled to have constant material thickness of 3 mm for the entire body. Because of its wide usage in aerospace industry the missile body is assumed to be aluminum which is a light and strong material. Also different from the AGARD wing, material properties for the missile are isotropic. Details of material properties and structural solution domain are given in Table 4-1 and Figure 4-7. CFD and CSD solution domain grid independence

studies for generic slender missile are not shown in this thesis since similar computational domains are used for missiles designed and developed by ROKETSAN, and the grid sizes used in this study are already proved to be fine enough for such missile geometries through several experimental comparisons.

Table 4-1 Material Properties of the Generic Missile

Material Property	Value
E	70 [GPa]
υ	0.35
ρ	2700 [kg/m^3]

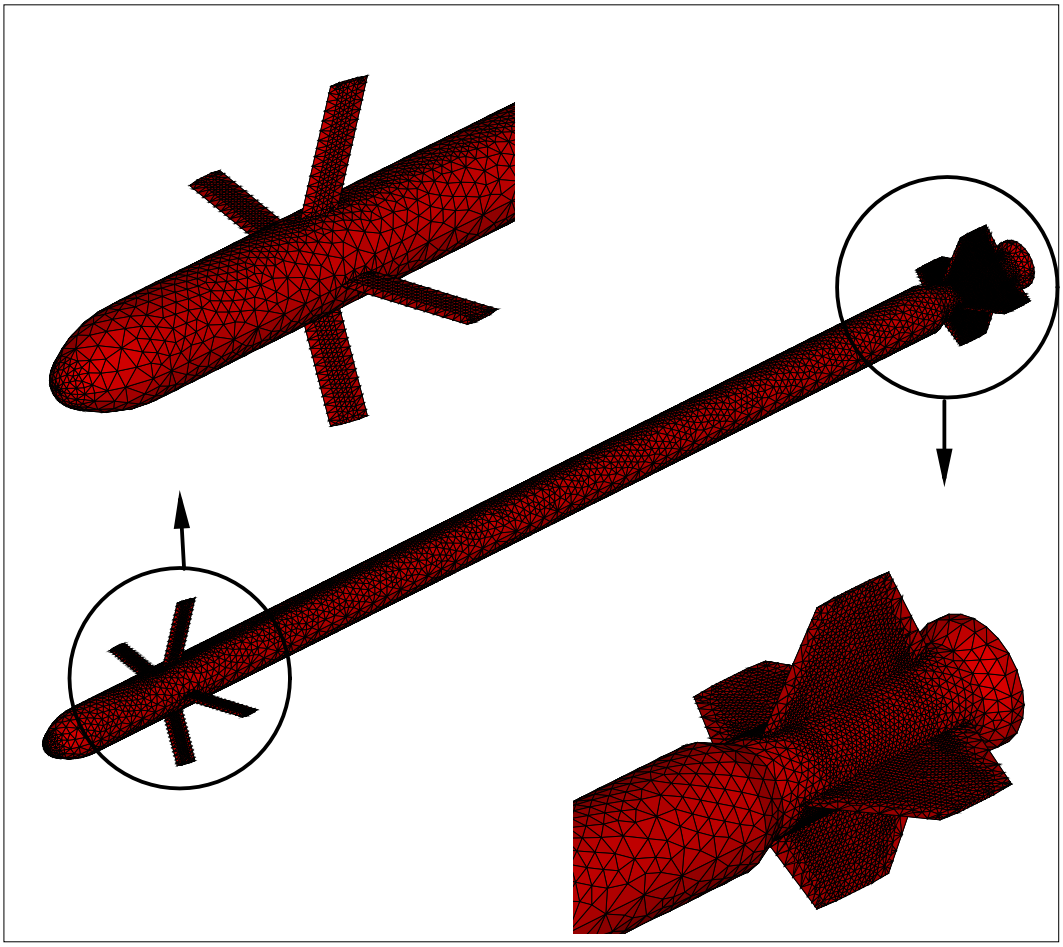

Figure 4-7 Structural Solution Domain

4.1 Results

Solution procedure for static aeroelastic analysis of missile geometry is the same as the one used for the AGARD wing analysis with the only difference being the convergence criterion. For generic slender missile analysis, convergence is declared when the absolute value of the maximum deformation difference between the last and previous iteration steps drops less than 1 % of the missile body thickness. Convergence history details are given in Table 4-2 and Figure 4-8. As it can be seen from Table 4-2, at iteration number 4, percent deformation difference between 4th and 3rd iteration steps dropped under 1 % and the analysis is stopped.

Table 4-2 Convergence History for the Aeroelastic Analysis of the Generic Missile

Iteration	Maximum Deflection [mm]	Absolute Difference [mm]	Percent Difference
1	14.01	-	-
2	13.52	0.48	16.1
3	13.57	0.05	1.4
4	13.56	0.01	0.2

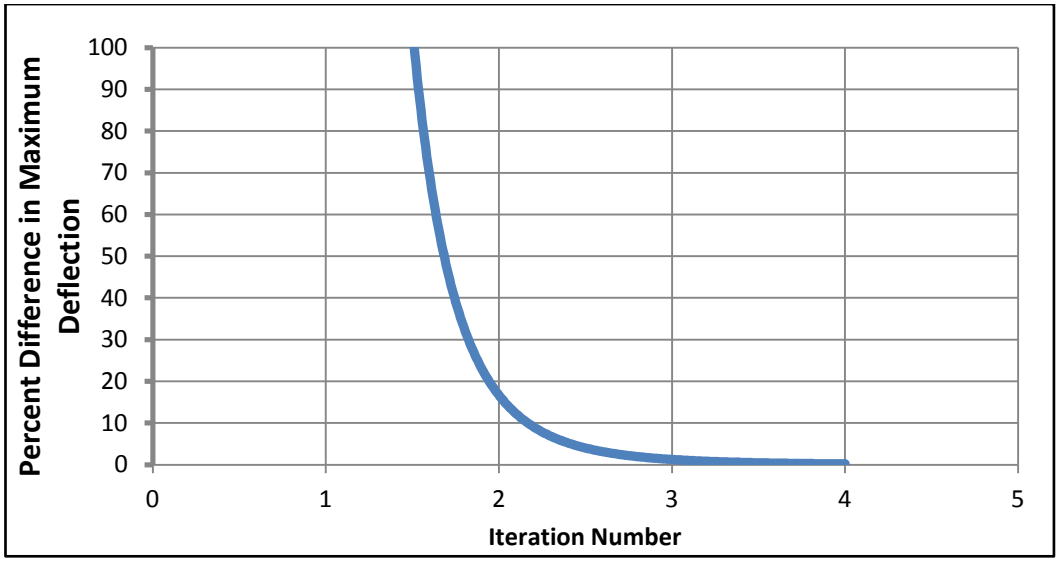

Figure 4-8 Convergence History for the Aeroelastic Analysis of the Generic Missile

Kriging interpolation method is used for data transfer processes in the analysis as described before. In Figure 4-9 contour plot of pressure distribution for fluid and structural grid is given. When the results of the interpolation process are investigated complete agreement between two solution domains is clearly observable.

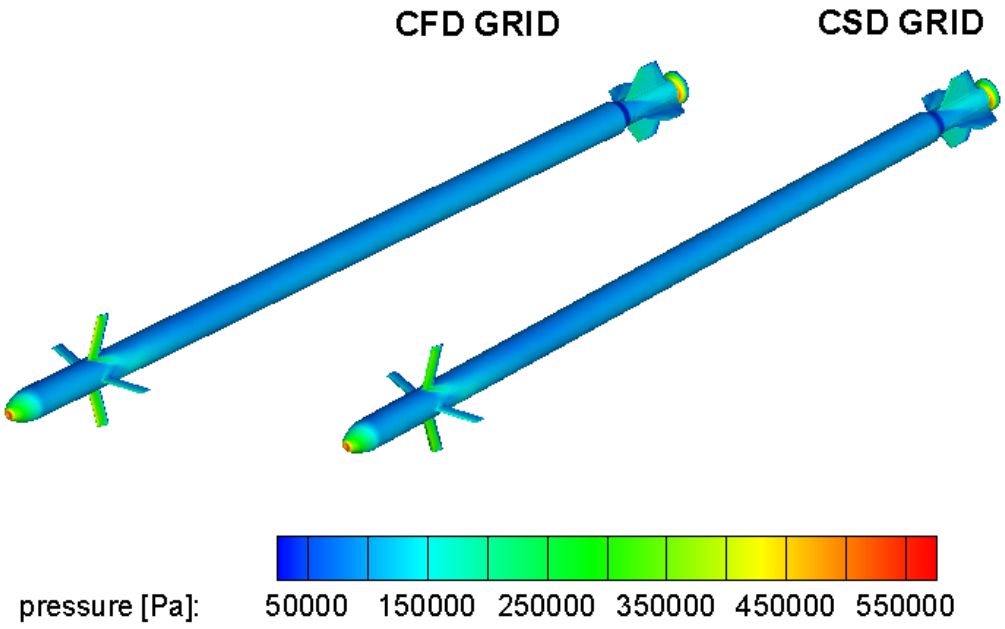

Figure 4-9 Missile Surface Pressure Distribution for CFD and CSD Domains

In order to understand the possible aeroelastic effects on a missile configuration, results of the generic slender missile is compared with the rigid one. First, the effects of aeroelasticity on total missile aerodynamics will be investigated. The sign convention used in the following parts of the thesis for aerodynamic forces and moments are given in Figure 4-10.

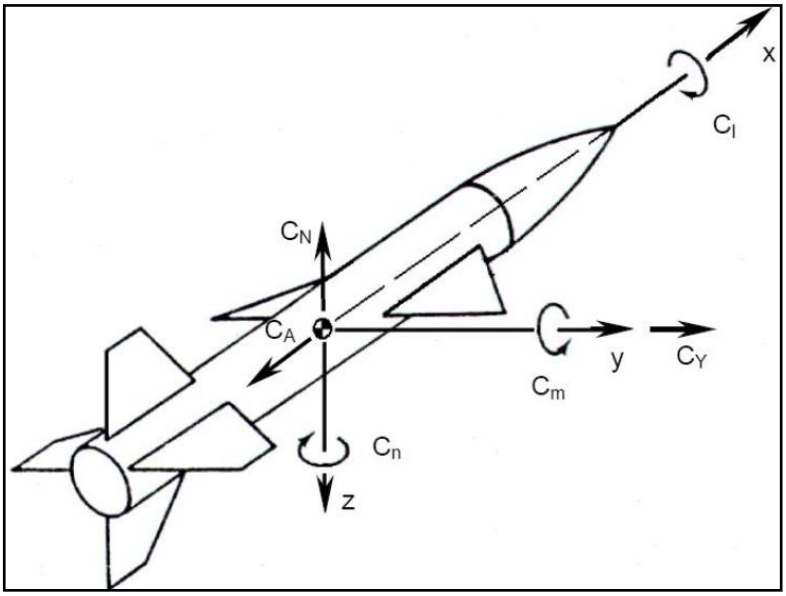

Figure 4-10 Missile Aerodynamic Sign Convention

Comparison of the aerodynamic performance parameters for rigid and elastic missiles is given in Table 4-3. Values for aerodynamic coefficients and parameters cannot be given due to privacy reasons. However, lift, drag, normal and axial force coefficients, pitching moment coefficient and center of pressure location results for elastic missile are compared with rigid missile results and at a first glance one can say that the aerodynamic performance of the missile is highly affected by aeroelastic phenomenon. When aerodynamic force coefficients are investigated, nearly 2 % drop in all coefficients can be seen for the elastic missile. Decrease in the lift and normal force coefficients indicates that the maneuvering capabilities of the missile are decreased. However pitching moment of the elastic missile is increased by approximately 10 %. This is due to the change in the center of pressure location of the missile. For the rigid missile, center of pressure is located in front of the moment reference point. The distance between center of pressure and moment reference location for elastic wing is increased by 12 %. In other words the stability of the missile is decreased by 12 % which is not desired.

Table 4-3 Total Missile Aerodynamics

Parameter	Percent Difference
C_L	-2.1
C_D	-2.0
C_N	-2.1
C_A	-2.0
C_M	9.7
$(X_{CP}-X_{CG})/D$	12.0

Contours of deformation rate for the entire missile for pitch plane are given in Figure 4-11. Due to the existence of angle of attack, nose and aft sections of the missile deform considerably. For canards, fin deflection angle increases the local angle of attack and hence pressure on canard number 2 and 4 increase accordingly.

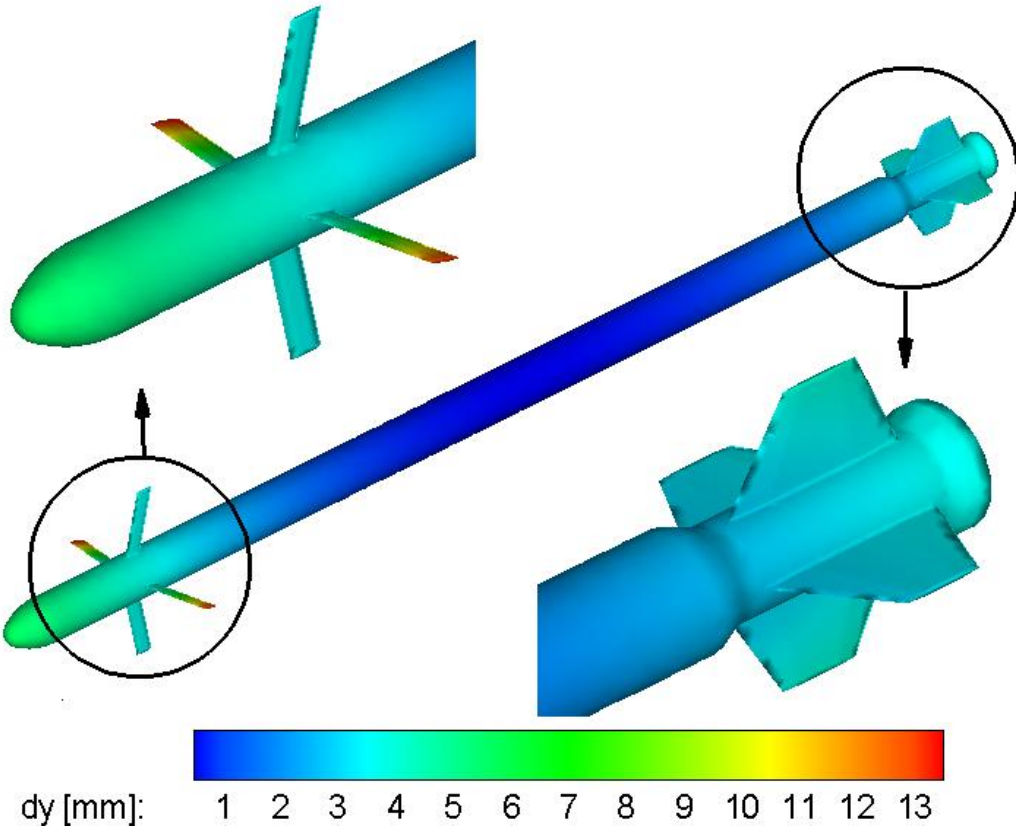

Figure 4-11 Deformed Missile after Aeroelastic Calculations

To understand the effects of aeroelasticity on the missile configuration deeper, canard and tail aerodynamics are investigated separately. In Table 4-4 results for canard aerodynamic parameters are compared for rigid and elastic missiles. Since canard number 1 and 3 are in the pitch plane, aerodynamic loads on these canards can be neglected when compared to canard number 2 and 4. Also since canard 2 and 4 are symmetric about the pitch plane, investigation of results for only canard 2 would be enough. When the results are compared for rigid and elastic missiles, lift force coefficient is decreased by 3.8 % and drag force coefficient is decreased by 6.6 % for the elastic missile. Also when the center of pressure location for this canard is investigated, one would see that the center of pressure location for elastic canard moves forward as much as 13 % of the root chord. These results indicate that the canard aerodynamic characteristics are highly changed by aeroelastic effects. Lift force generated by the canards is decreased. Also center of pressure location changed by 13 % of root chord length that if the hinge line design is completed using only rigid case. Due to aeroelastic effects hinge moment on the canards may go beyond the design hinge moment range and flight of the rocket can result with catastrophic failures. An illustration of canards for rigid and elastic cases is also given in Figure 4-12.

Table 4-4 Changes in Canard Aerodynamics

Parameter	Percent Difference
C_L	-3.8
C_D	-6.6
X_{cp}/C_{root}	-13.0

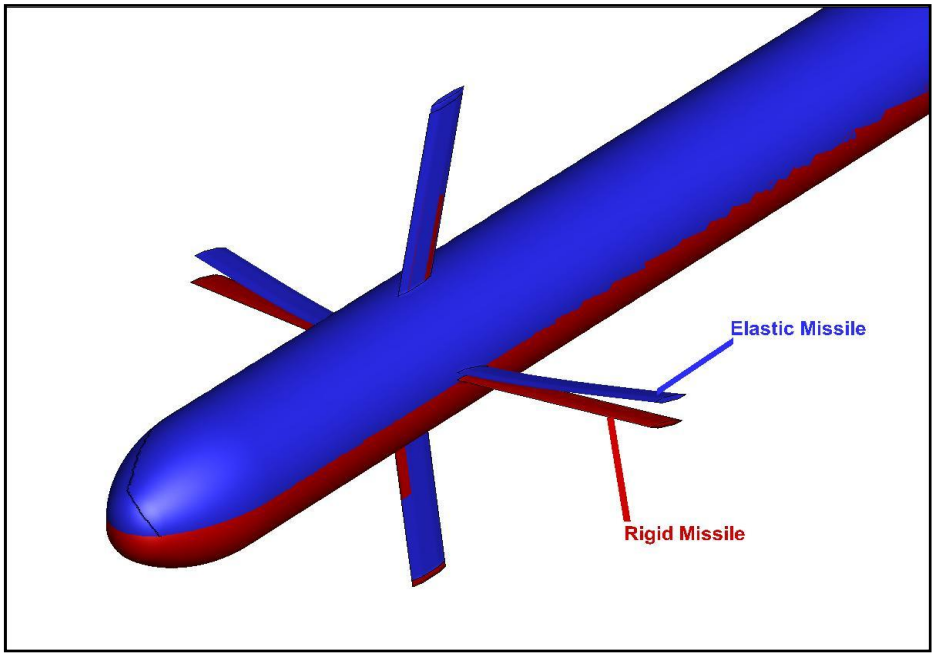

Figure 4-12 Rigid and Deformed Elastic Canards

Tail aerodynamic loads for rigid and elastic missiles are also compared. Results for only tail 2 are given due to the same reasons with the canards. One can see from Table 4-5 that tail aerodynamic characteristics are not affected as much as canard aerodynamic characteristics. But for tails considerable changes in aerodynamic performance is also present. Lift and drag force coefficients are decreased by 2.6 and 5.3 %, respectively. But center of pressure location is approximately same for both cases. An illustration of tails for rigid and elastic cases is given in Figure 4-13.

Table 4-5 Changes in Tail Aerodynamics

Parameter	Percent Difference
C_L	-2.6
C_D	-5.3
X_{cp}/C_{root}	0.1

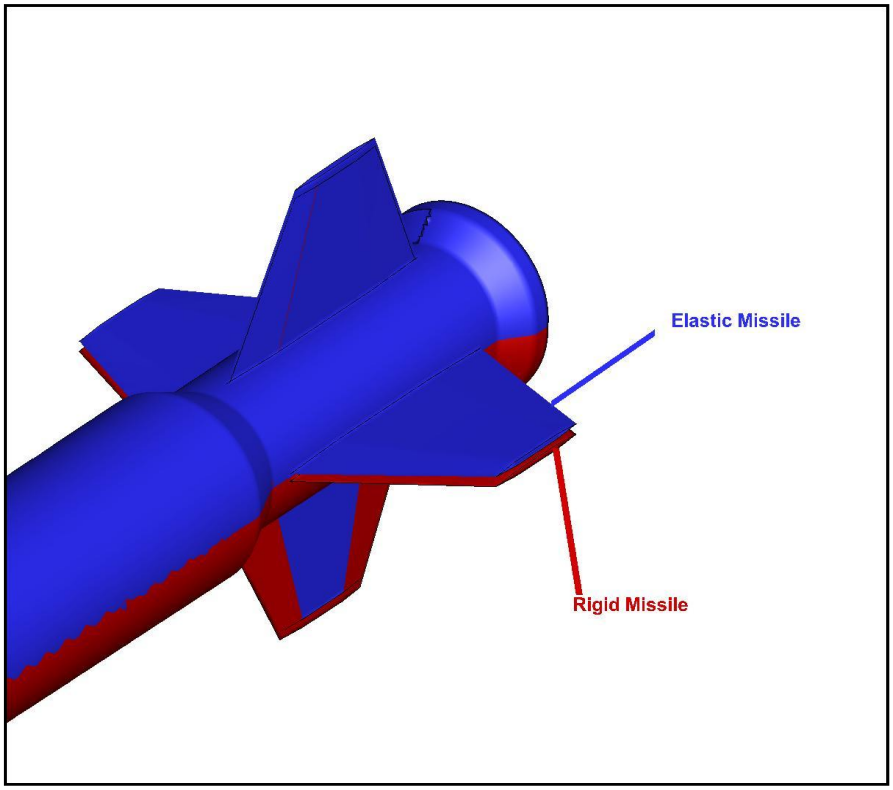

Figure 4-13 Rigid and Deformed Elastic Tails

4.2 Conclusions

Static aeroelastic analysis for a generic slender missile geometry is conducted in order to investigate possible effects of aeroelasticity on rocket or missile configurations. Results of the analysis for elastic missile are compared with the rigid case.

Generic slender missile is a canard controlled configuration, geometry of which is similar to a conventional 2.75" rocket geometry. In the aeroelastic analysis of the missile the same procedure with AGARD 445.6 wing is used except the convergence criteria. CFD and CSD domains have 3,240,611 and 238,697 tetrahedral elements, respectively. Aeroelastic analysis converges at 4 aeroelastic iterations. When aerodynamic force coefficients are investigated, approximately 2 % drop in all aerodynamic force coefficients can be seen for the elastic missile. Pitching moment

of the elastic missile is increased by approximately 10 %due to the change in center of pressure location. The distance between center of pressure and moment reference location for elastic missile is increased by 12 %. In other words the stability of the missile is decreased by 12 %.

When the aerodynamic loads on canard 2 are compared for rigid and elastic missiles, lift and drag force coefficients are decreased by 3.8 and 6.6 %, respectively and the center of pressure location of elastic canard moves forward by 13 % of the root chord length. Considerable changes in aerodynamic performance are also present for tails. Lift and drag force coefficients are decreased by 2.6 and 5.3 %, respectively. But for tail 2, center of pressure location is approximately the same for both cases.

Deformations in canards and tails reduce the lift force produced by these fin sets. This reduction in lift force may result in reduced control effectiveness and maneuverability. Also stability characteristics of the missile changes due to deformations. For this generic missile, stability is decreased considerably compared to the rigid case. Deformations in the control surfaces also change the center of pressure location at the fins which may cause high hinge moments around the hinge line. As a result enough power may not be produced to control the missile aerodynamically.

CHAPTER 5

CONCLUSIONS AND FUTURE WORK

In this thesis a loosely coupled fluid-structure interaction analysis method for the solution of static missile/rocket aeroelastic problems was developed by using commercial codes FLUENT and ANSYS. First the subject is introduced, secondly methodology and governing equations used in the study are explained, thirdly analysis for a test case was conducted and compared with references and finally a generic slender missile geometry is analyzed for static aeroelastic effects.

AGARD 445.6 wing is used as the test case in order to investigate whether the developed loosely coupled fluid-structure analysis method works or not. For weakened AGARD 445.6 wing grid independence studies are conducted for both fluid and structure solution domains. For the given flight conditions as a result of aeroelastic analysis lift force coefficient of the wing decreases dramatically compared to rigid wing because of the twist motion that the wing makes for elastic case. Due to twist motion, local angle of attack of the wing decreases along the wing span which highly affects and reduces the aerodynamic performance of the wing. The static aeroelastic analysis results for weakened AGARD 445.6 wing are compared with the reference studies of Cai [9]. Leading and trailing edge deformations and pressure coefficient results for two span locations are in good agreement with this reference study. Solution of this test case and the compared

results shows that the developed loosely coupled fluid-structure interaction analysis method can be applicable for static fluid-structure interaction problems.

To investigate possible effects of aeroelasticity on rocket or missile configurations, static aeroelastic analysis for a canard controlled generic slender missile which is similar to a conventional 2.75" rocket geometry is conducted and results of the analysis for elastic missile are compared with rigid case. Reduction in all aerodynamic force coefficients can be seen for elastic missile when the results are investigated for total missile aerodynamics. Pitching moment of the elastic missile is increased considerably due to the change in center of pressure location. Also the distance between center of pressure and moment reference location for elastic missile is increased and hence stability of the missile is decreased dramatically. When the aerodynamic loads on canards are compared for rigid and elastic missiles, lift force and drag force coefficients decreases slightly whereas center of pressure location for elastic canards change significantly. For tails, aerodynamic coefficients are reduced to some extent but center of pressure location is approximately same for rigid and elastic cases.
For an elastic missile or rocket geometry following conclusions can be reached:

- Lift force produced by canards and tails lessen due to deformations in these fin sets as a result of which control effectiveness and maneuverability of the configuration reduce.
- By reason of deformations, stability characteristics of the missile changed significantly. For this generic missile, stability decreased greatly compared to rigid case.
- Center of pressure locations for canards also change because of deformations in the control surfaces which may cause high hinge moments around hinge line during flight thus control mechanism of the missile may not produce enough power to control the missile aerodynamically.

As future work, firstly the developed method will be validated with more test cases and experimental data if available. For structural model, use of elements having mid-nodes would increase the accuracy of the result. These mid-node elements can be handled in the future versions of this method. Steady state fluid-structure interaction simulation procedure will be automated by future developed computer code. Also development of a closely coupled steady state and transient fluid-structure interaction solution method is planned. When this method is developed, aeroelastic effects on rockets and missiles would be investigated deeper.

REFERENCES

[1] Kroyer, R. *"FSI Analysis in Supersonic Fluid Flow"*, Computers and structures 81 (2003) 755-764

[2] Guruswamy, G. P. *"A Review of Numerical Fluids/Structures Interface Methods for Computations using High-Fidelity Equations"*, Computers and Structures, v. 80, pp. 31-41.

[3] Hübner B., Walhorn E., Dinkler D. *"A Monolithic Approach to Fluid-Structure Interaction Using Space-Time Finite Elements"*, Comput. Methods Appl. Mech. Engrg. 193 (2004) 2087-2104

[4] Kamakoti, R., Shyy, W. *"Fluid- Structure Interaction for Aeroelastic Applications"*, Progress in Aerospace Sciences 40 (2004) 535-558

[5] Liu, F., Cai, J., Zhu, Y.,Tsai. H., Wong, A. *"Calculation of Wing Flutter by a coupled Fluid-Structure Method",* Journal of Aircraft vol. 38, no. 2, March-April 2001

[6] Slone, A., Pericleous, K., Bailey, C., Cross, M. *"Dynamic Fluid-structure Interaction Using Finite Volume Unstructured Mesh Procedures"*, Computers and Structures 80 (2002) 371-390

[7] Lesoinne, M., Sarkis, M., Hetmaniuk, U., Farhat, C. *"A Linearized Method for the Frequency Analysis of Three Dimensional Fluid/Structure Interaction Problems*

in All Flow Regimes", Computer Methods in Applied Mechanics and Engineering 190 (2001) 3121-3146

[8] Zwaan, R., Prananta, B. *"Fluid/Structure Interaction in Numerical Aeroelastic Simulation"*, International Journal of Non-Linear Mechanics 37 (2002) 987-1002

[9] Cai J., Liu F., Tsai H.M., Wong A.S.F., *"Static Aero-elastic Computation with a Coupled CFD and CSD Method"*, AIAA 2001-0717, Aerospace Sciences Meeting and Exhibit, 39th, Reno, NV, Jan. 8-11, 2001.

[10] Sümer, B. *"Fluid Structure Coupled Analysis of an Aerodynamic Surface"*, Ms. Thesis, Middle East Technical University, 2004

[11] Başkut, E. *"Closely Coupled Approach for Static and Dynamic Aeroelastic Problems"*, Ms. Thesis, Middle East Technical University, 2010

[12] Yates, E. C., *"AGARD standard aeroelastic configurations for dynamic response I-wing 445.6"*, AGARD Report 765, North Atlantic Treaty Organization, Group for Aerospace Research and Development, 1988.

[13] *"ANSYS FLUENT Theory Guide"*, 2009

[14] Anderson, J., D., *"Modern Compressible Flow"*, McGraw and Hill, 1991

[15] *"ANSYS, Inc. Theory Manual"*, 1994

[16] White, F., M., *"Viscous Fluid Flow"*, McGraw and Hill, 1991

[17] *"FLUENT 6.3 Documentation"*, 2006

[18] Chorin, A., J., *"Numerical Solution of Navier-Stokes Equations"*, Mathematics of Computations, 22:745-762, 1962

[19] *"ANSYS Structural Analysis Guide"*, 2004

[20] Benko, R., J., *"FLUENT Overview for Solving FSI Problems"*, 2006 CFD Submit, 2006

[21] Stein, M., L., *"Interpolation of Spatial Data: Some Theory for Kriging"*, Springer-Verlag, New York, 1999

[22] *"Tecplot 360 User's Manual"*, 2011

[23] Davis, J. C., *"Statistics and Data Analysis in Geology, Second Edition"*, John Wiley and Sons, New York, 1973, 1986